Activation of the epidermal growth factor receptor (EGFR) by redox cycling and alkylating quinones: Mechanisms and consequences

Inaugural-Dissertation
zur

Erlangung des Doktorgrades der Mathematisch-Naturwissenschaftlichen Fakultät der Heinrich-Heine-Universität Düsseldorf

vorgelegt von

Kotb Abdelmohsen

aus Ägypten

Düsseldorf
2003

Gedruckt mit der Genehmigung der

Mathematisch-Naturwissenschaftlichen

Fakultät der Heinrich-Heine-Universität Düsseldorf

Tag der mündlichen Prüfung: 11.12.2003

Referent: Prof. Dr. Dr. Helmut Sies

Korreferent: Prof. Dr. Hans-Dieter Martin

Contents

Acknowledgements

This work was carried out in the Institut für Biochemie und Molekularbiologie I, Heinrich-Heine Universität, Düsseldorf, Germany.

I am greatly indebted to Professor Dr. Dr. Helmut Sies for giving me the opportunity to perform my Ph.D. studies in his great institute, his ideas and critical discussions.

I owe my sincere thanks to Prof. Dr. Martin for taking over the Korreferat, his fruitful discussions about quinones and for his organic chemistry course.

I am deeply grateful to my supervisor, PD. Dr. Lars Oliver Klotz, who introduced me the exciting field of signal transduction and has patiently instructed and encouraged me during the course of these studies. Under his guidance all facilities in his laboratory were placed at my disposal. There is no way to thank him in words for what I have learned from him.

My special thanks go to PD. Dr. Peter Brenneisen for his constructive criticism and valuable suggestions. I have had the pleasure to cooperate with his group through working with Dominik Stuhlmann, whom I thank for expert work on microinjection.

I thank all former members of the institute, in particular Dr. Darius Buchczyk**,** and Dr. Peter Schröder for their help and encouragements. I thank Marko Döll for teaching me the glutathione assay and Dr. Elena Ostrakhovitch for her fruitful discussions.

My warm and sincere thanks go to each and every member of the Institut für Biochemie und Molekularbiologie I, for their support during the past years and for creating a very nice working and cooperating atmosphere. In particular, I express my thanks to Arne Gerber, Claudia von Monfort, Pauline Patak and Dr. Niloofar Nilo Ale-Agha for having a unique scientific cooperation. I deeply thank Prof. Stahl, Dr. Olivier Aust, Dr. Antonio Pérez-Gálvez, Ira Melcheier, Jule Beier, Cristy Ramos, Andrea Borchardt, Alejandro Betancor, Felicitas Daubrawa, Peter Graf, and Heide Krahl for their help and support.

My warm thanks to Elisabeth Sauerbier for her expert technical assistance and teaching me immunohistochemistry.

My thanks are due to Prof. Dr. Schewe for his fruitful discussions and Dr. Holger Steinbrenner for valuable discussions and keeping me aware that life exists also outside the laboratory.

My thanks are due to Marlies Scholtes for her professional administrative services and supporting me with all official information I needed.

My thanks are due to DFG (SFB575/B4) for supporting this work and giving me the opportunity to open my scientific horizon by attending several conferences to be able to get a view of the international world of Science.

Finally, I express my deepest gratitude to my family members in Cairo (Egypt), my parents, my brother, my sister and their wounderful kids.

Düsseldorf, November 2003

Kotb Abdelmohsen

Abbreviations

APS	Ammonium persulfate
BQ	*p*-Benzoquinone
DEM	Diethyl maleate
DMEM	Dullbecco's Modified Eagle's Medium
DMNQ	2,3-Dimethoxy-1,4-naphthoquinone
DMSO	Dimethylsulfoxid
Dox	Doxorubicin
DTT	1,4-Dithiothreitol
EGF	Epidermal growth factor
EGFR	Epidermal growth factor receptor
ERK 1 and ERK 2	Extracellular signal-regulated kinase- 1 and 2
ERK5	Extracellular signal-regulated kinase-5
FCS	Fetal calf serum
GJC	Gapjunctional intercellular communication
GSSG	Glutathione disulfide
MAPK	Mitogen-activated protein kinase
MMC	Mitomycin C
MQ	Menadione 2-methyl-1,4-naphtoquinone.
MTT	4,5-Dimethylthiazol-2-yl-2,5-diphenyl-2H-tetrazolium bromide
NAC	N-Acetyl cysteine
NAD(P)H	Nicotinamide adenine dinucleotide (phosphate), reduced
NQOR-1	NAD(P)H:quinone oxidoreductase-1
NR	Neutral red , 3-amino-7-dimethyl-2-methylphenazine
PI3K	Phosphoinositide 3-kinase
PTPase	Protein tyrosine phosphatase
ROS	Reactive oxygen species
SDS	Sodium dodecyl sulfate
SOD	Superoxide dismutase
TEMED	N,N,N',N'-Tetramethylethylendiamin
TPA	12-O-Tetradecanoylphorbol-13-acetat
Tris	Trishydroxymethylaminomethan

1. Introduction

1.1. Quinones in biochemistry and medicine

Quinones are involved in a number of biochemical reactions (Bolton et al., 2000). These include redox reactions such as (i) the transport of electrons by ubiquinol in the mitochondrial respiratory chain, (ii) the carboxylation of blood coagulation factors involving the K vitamins, or (iii) redox cycling as a result of quinone reduction followed by reoxidation with molecular oxygen, concomitantly generating the superoxide anion (Brunmark and Cadenas, 1989, and Suttie, 1985). Further, a variety of alkylation reactions are observed, including Michael-type additions of sulfhydryl groups to quinones (Boatman et al., 2000) or DNA alkylation (Hargreaves et al., 2000, and Arif et al., 2003). For example, certain quinones are known to form cysteinyl adducts with hemoglobin and albumin in F344 rats that are not detected in control animals (Waidyanatha, 2002).

Three quinones with different structures and reactivities were used in this study (Figure 1.1). Menadione (MQ; 2-methyl-1,4-naphtoquinone), an alkylating and redox-cycling compound, *p*-benzoquinone (BQ), a strongly alkylating quinone, and 2,3-dimethoxy-1,4-naphthoquinone (DMNQ), an exclusive redox-cycler.

Menadione is a naphthoquinone derivative that has been used clinically because of its vitamin K-like properties (it is also termed vitamin K_3). It is enzymatically converted to menaquinone-4 (2-methyl-3-geranyl-geranyl-1,4-naphthoquinone, a form of vitamin K_2) by mammals (Taggart and Matschiner, 1969). As it is easily synthesised chemically (Mayer 1971), it was regarded a suitable source of vitamin K. Due to its unsubstituted position at C-3, however, menadione has alkylating properties, accounting for side-effects such as thiol depletion that may ultimately mediate cytotoxicity. For this reason, it is no longer recommended as a dietary vitamin K supplement, although menadione is still commonly used in animal diets, partly in water-soluble form, e.g. as menadione sodium bisulfite, and is frequently used as a model quinone in cell culture studies.

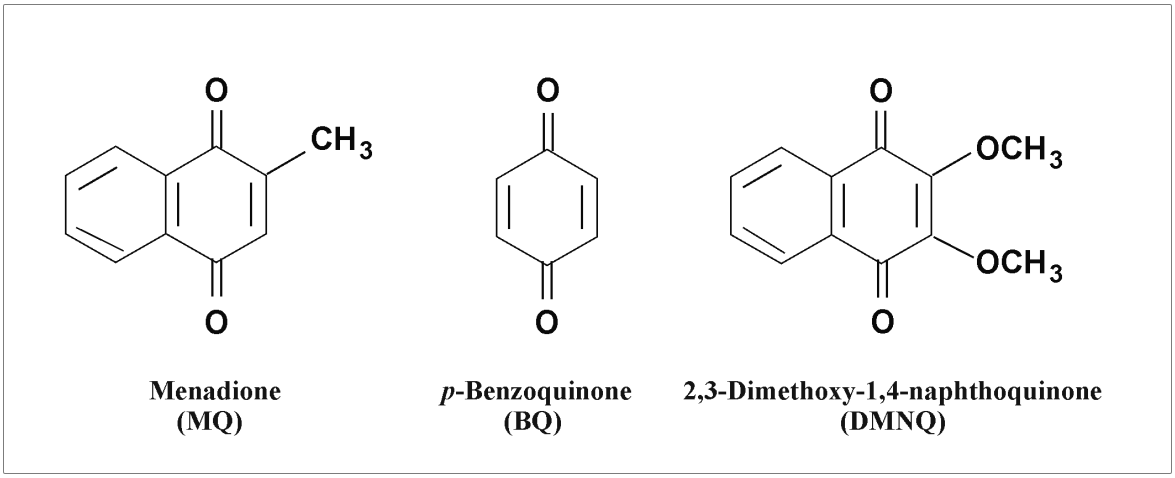

Figure 1.1. Chemical structures of model quinones

It is the cytotoxicity of menadione, however, that has rendered it as an interesting lead compound for the development of chemotherapeutics (Carr et al., 2002). Indeed, menadione was demonstrated to potently kill cultured cancer cells and was employed in animal studies as well as in preliminary clinical studies (Nutter et al., 1991, and Tetef et al., 1995).

DMNQ is known to be a pure redox cycler and cannot perform alkylation reactions due to its C-3 being blocked (Gant et al., 1988). In contrast to DMNQ, BQ as well as MQ are strongly alkylating agents targeting many cellular proteins such as nucleophosmin, galectin-1, protein disulfide isomerase, Hsp60 or Hsp70 (Lame et al., 2003).

One of the first compounds tested for antitumor activity by the National Cancer Institute (NCI) of the USA in 1955 was a simple redox active quinone, methyl-*p*-benzoquinone. Doxorubicin (Dox) and mitomycin C (MMC) (Figure 1.2) are quinones that are widely used as drugs in cancer chemotherapy nowadays.

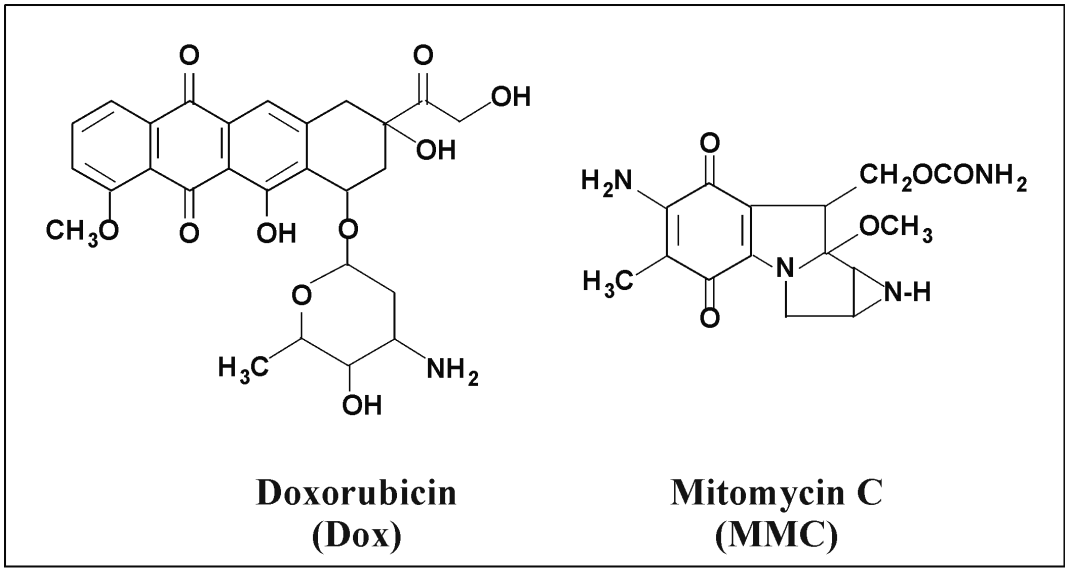

Figure 1.2. Chemical structures of chemotherapeutic quinones: doxorubicin and mitomycin C

Doxorubicin is an anthraquinone derivative derived from *actinomycetales sp*. and is used as an antitumor drug in the treatment of various human cancers such as acute leukemia, as well as solid tumors including breast, ovarian, or endometrial cancers (for reviews, see Calabresi and Chabner, 1996, and Chabner et al., 1996)

Although the principle mechanism(s) of the antitumor activity of doxorubicin is not fully understood, three mechanisms were proposed: (i) one or two electron reduction with generation of the doxorubicin-semiquinone radical or the hydroquinone (Bruce, 1981, and Malisza and Hasinoff, 1996) that react with oxygen to produce reactive oxygen species and ultimately damage the DNA and other cellular components such as proteins and the cell membrane (Reiter, 1997, and Miral, 1998), (ii) intercalation of the planar structure of doxorubicin with DNA, leading to inhibition of RNA and DNA synthesis, and (iii) inhibition of topoisomerase II (Huimin et al., 2001, and Tero et al., 2000), a key enzyme in DNA replication.

MMC is an effective antitumor drug, derived from *streptomyces sp.* And used in treatment of various cancers, including gastrointestinal, pulmonary and breast cancer (Garewal, 1988, and Pasterz, 1985). MMC can be metabolized to an active species which crosslinks complementary DNA strands, thereby inhibiting DNA synthesis (Dorr 1988). Guanine was found to be the preferred site of alkylation of DNA by MMC (Tomasz et al., 1988).

The flavoenzyme NAD(P)H:quinone oxidoreductase-1, NQOR-1, formerly known as DT-diaphorase (Ernster and Navazio, 1958, and Ernster et al., 1962), catalyzes the two-electron reduction of various quinones at the expense of NAD(P)H.

The resulting hydroquinones can be oxidised in the presence of O_2, generating superoxide anion radicals that are converted to H_2O_2 by superoxide dismutase (SOD). H_2O_2 can then be reduced to water at the expense of glutathione by glutathione peroxidase (see 1.2 below).

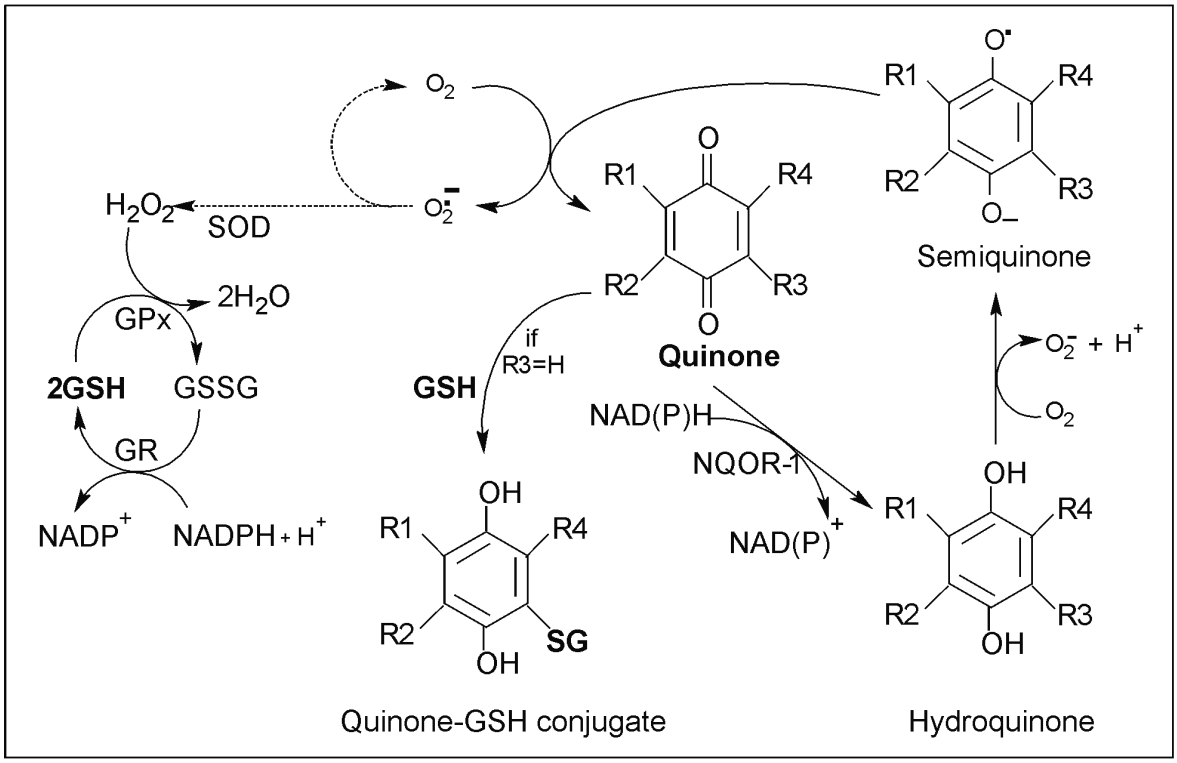

Figure 1.3. Quinone metabolism

Pathways of quinone metabolism show the involvement of glutathione. When R3 = H as in the cases of MQ and BQ a quinone-GSH is formed (see text). GSH = glutathione. SOD = superoxide dismutase. GPx = glutathione peroxidase, GR = glutathione reductase.

1.2. Glutathione

The tripeptide glutathione (GSH, γ-glutamyl-cysteinylglycine) is the major intracellular low molecular weight sulfhydryl compound in animals, plants and in most microorganisms (for review, see Sies, 1999, and Meister and Anderson, 1983).

In mammalian cells glutathione is synthesised from its constituent amino acids in two steps (Figure 1.4). First, L-glutamate and L-cysteine are conjugated to form γ-glutamylcysteine in a reaction catalyzed by γ-glutamylcysteine synthetase. The second step is catalyzed by glutathione synthetase, which catalyzes the formation of a peptide bond between glycine and γ-glutamylcysteine.

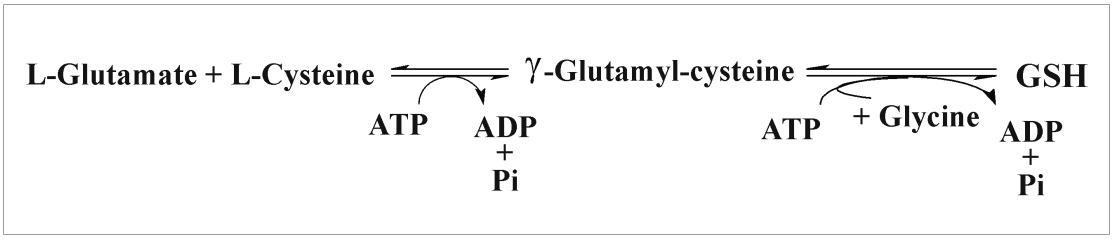

Figure 1.4. Synthesis of glutathione from its constituent amino acids

The level of glutathione in mammalian tissues, particularly the liver, usually is in the millimolar range and within the cell less than 10 % of glutathione is in the disulfide form (GSSG) (Akerboom et al., 1982). GSH can undergo a non-enzymatic conjugation with electrophilic compounds *via* its sulfhydryl group. However, this conjugation is greatly facilitated by glutathione S-transferases.

Glutathione is found to be involved in both akylation and redox cycling of quinones (Ernster, 1986, and Ann, 1986). For instance, GSH reacts directly with benzoquinone in a Michael-type addition whereas NQOR-1 catalyses two electron reduction of DMNQ, which may be followed by the generation of reactive oxygen species (ROS) that are further scavenged by GSH (Figure 1.3).

1.3. Quinone-induced signaling

Cells respond to extracellular stimuli such as those imposed by xenobiotic quinones by activating stress-responsive intracellular signaling cascades that regulate cellular proliferation and survival. These include pathways activated by DNA damage, such as p53-related events (Wu. R. et al., 1998) and general stress-responsive cascades, such as mitogen-activated protein kinase (MAPK) cascades, the phosphoinositide 3-kinase (PI3K)/Akt cascade (see below) and others (Li et al., 2001, and Klotz et al., 2002b).

Not only are intracellular signaling pathways affected that regulate the survival and proliferation of the respective cell harboring these signaling cascades, but a stress-response may also consist of disconnecting a cell from its environment, e.g. by downregulation of gap junctional intercellular communication (GJC, see below) in order to prevent diffusion of xenobiotics or toxic metabolites thereof within a tissue (Figure 1.5).

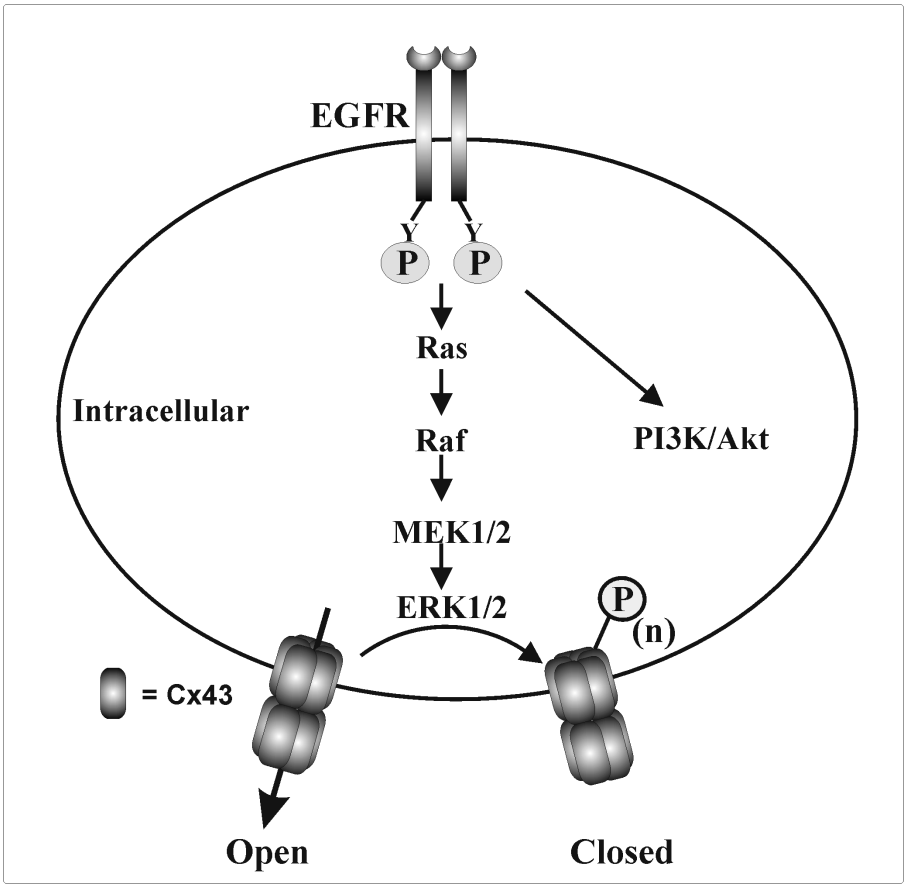

Figure 1.5. EGFR-dependent signaling: from intracellular to intercellular communication

1.3.1 Epidermal growth factor receptor-dependent signaling

The pidermal growth factor (EGF) receptor (EGFR) (also known as HER1 or ErbB1) is a transmembrane glycoprotein (170 kDa) composed of an extracellular ligand-binding domain, a transmembrane lipophilic segment, and an intracellular domain with protein tyrosine kinase activity (Cadena and Gill 1992). The EGF receptor family is comprised of four members: the EGFR itself (ErbB1/EGFR/HER1), ErbB2 (HER2/neu), ErbB3 (HER3), and ErbB4 (HER4) (Baselga 2002, Ciardiello et al., 2001 and Olayioye et al., 2000).

EGFR family members are overexpressed in one third of all epithelial cancers including non-small cell lung cancer (NSCLC), head and neck, breast, gastric, prostate, ovarian, colorectal carcinoma and glioblastoma (Agus et al., 2000, Prenzel et al., 2001 and Mendelsohn 2002).

Activation of the receptor occurs upon binding of its ligand, such as the epidermal growth factor (EGF), to the extracellular domain. This causes the receptor to dimerize with either another EGFR monomer or with another member of the ErbB family (Sako et al., 2000). Receptor dimerization is followed by phosphorylation of tyrosine residues within the cytoplasmic domain (Figure 1.6), recruitment and phosphorylation of several intracellular substrates (Figure 1.5), leading to mitogenic signaling and the stimulation of cellular activities linked to growth and proliferation (Alroy and Yarden, 1997).

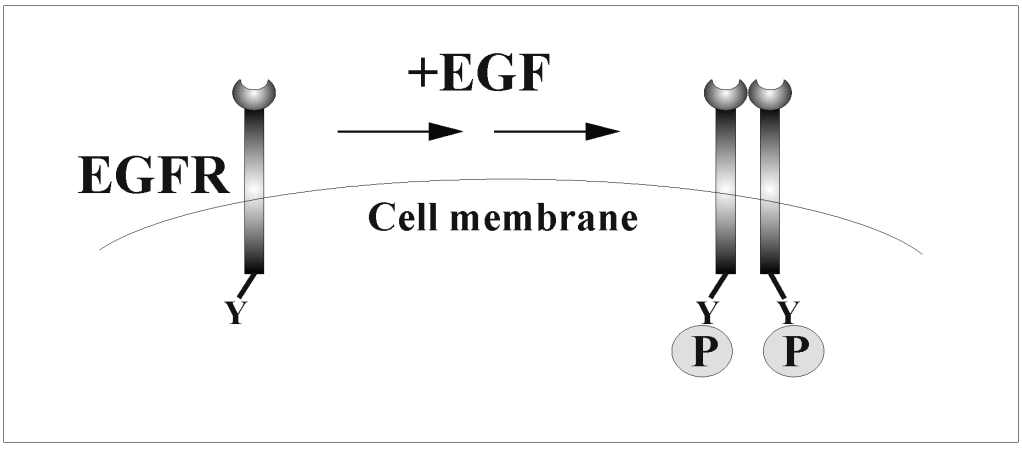

Figure 1.6. Dimerization of epidermal growth factor receptor (EGFR) and tyrosine phosphorylation induced by the epidermal growth factor (EGF)

Activation of EGFR leads to activation of a MAPK family subgroup, the extracellular signal-regulated kinase (ERK) 1 and ERK 2 *via* Ras (Aronheim et al., 1994), Raf (Marais 1995) and MEK1/2 (Dent 1992) (Figure 1.5). ERK1/2 is activated by phosphorylation of its conserved threonine and tyrosine residues on a Thr-X-Tyr-motif (Ahn et al., 1992). Extracellular stimuli such as menadione as well as hydrogen peroxide, or peroxynitrite have been shown to intensely activate the ERK pathways at the level of the EGF receptor (Klotz, 2002a, and Klotz et al., 2002b).

In addition to ERK1/2, ERK5 is another member of the MAPK family and its activity, required for proliferation (Kato et al., 1998), is stimulated with agents known to activate receptor tyrosine kinases, such as EGF (Mody et al., 2001). Another pathway emanating from the EGFR is the PI3K/Akt cascade (Figure 1.5). Akt, also known as protein kinase B (PKB), is a serine/threonine protein kinase, originally identified as the product of the oncogene *v*-akt of the acutely transforming retrovirus AKT8 (Bellacosa et al., 1991) and is known to promote cell survival in several cell lines (Henryk et al., 1997, Goswami et al., 1999, Kulik et al., 1997, Lee and Juliano, 2000).

1.3.2 Gap junctions

Cell-to-cell communication (Loewenstein, 1987) through gap junctional channels (GJC: gap junctional communication) is essential for the development and maintenance of animal tissues. These channels consist of two connexin hexamer hemi-channels (Figure 1.7*A*) (for review, see Toon et al., 2001) to connect the cytoplasms of two adjacent cells, allowing the diffusion of low molecular weight compounds (< ca. 1 kDa), including cyclic AMP (cAMP) and inorganic ions such as Ca^{2+}in a process known to be regulated by phosphorylation of the gap junctional proteins, the connexins (Figure 1.6) (Willecke et al 2002, and Unger et al., 1999). Gap junctional channels can be homotypic, consisting of two identical (homo- or heteromeric) connexons, or heterotypic with two different types of connexons (Figure 1.7*B*).

GJC has been hypothesized to play a crucial role in the regulation of carcinogenesis, because (i) many tumor cells display low levels of GJC (Trosko et al., 1998), (ii) many tumor promotors such as TPA, 12-*O*-tetradecanoylphorbol-13-acetate (Oh et al., 1991) are known to decrease GJC and (iii) connexin-32 knockout mice have higher tendency to develop liver cancer than their control counterparts (Temme et al., 1997).

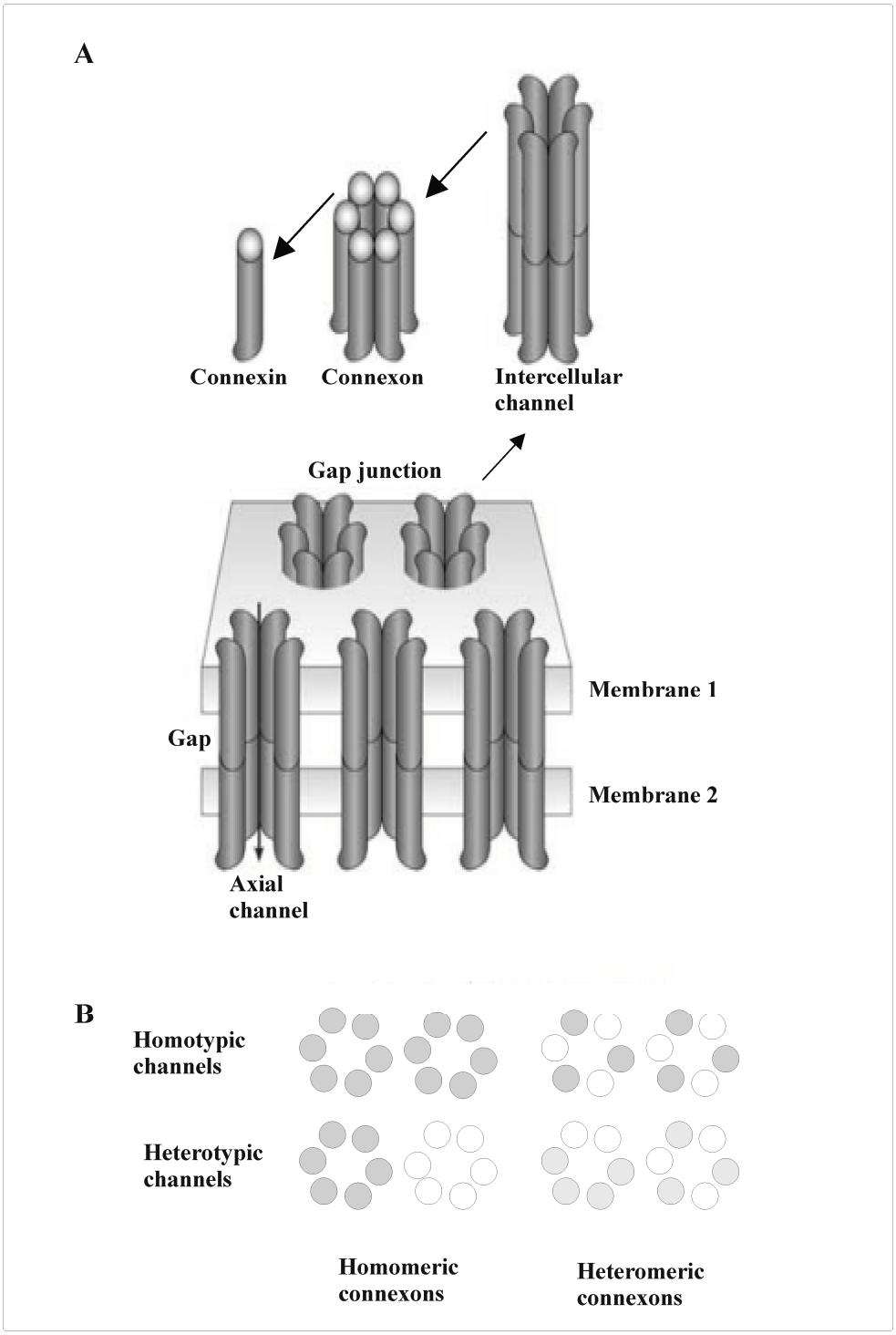

Figure 1.8. Structural model of Gap Junction Channels

(A) Several gap junctional channels, interconnecting two cells. Each cell contributes a hemichannel (connexon) to the complete gap junction channel. Each connexon is composed of six connexin subunits, adapted from Goodenough and Paul, 2003.

.(B) Homotypic gap junctional channels consist of two identical (homo-or heteromeric) connexons, whereas heterotypic channels are built of two different types of connexons.

GJC can be downregulated by phosphorylation of connexin-43 that is mediated by ERK1/2 (Lampe and Lau 2000). Expectedly, ERK1/2 activation induced by menadione indeed resulted in downregulation of GJC (Klotz et al., 2002b). In addition to ERK1/2, ERK5 was recently shown to be another connexin kinase (Scott at al., 2003).

Connexin phosphorylation usually results in loss of GJC (Lampe and Lau, 2000, and Kim et al., 1999). Connexin-43, the major connexin in the cell line employed in this study, may be phosphorylated by ERK1/2 on three sites, Ser255 as well as Ser279/Ser282, all of which are located in the C-terminal cytoplasmic domain of the protein (Figure 1.9) (Warn-Cramer et al., 1996, and Lampe and Lau, 2000).

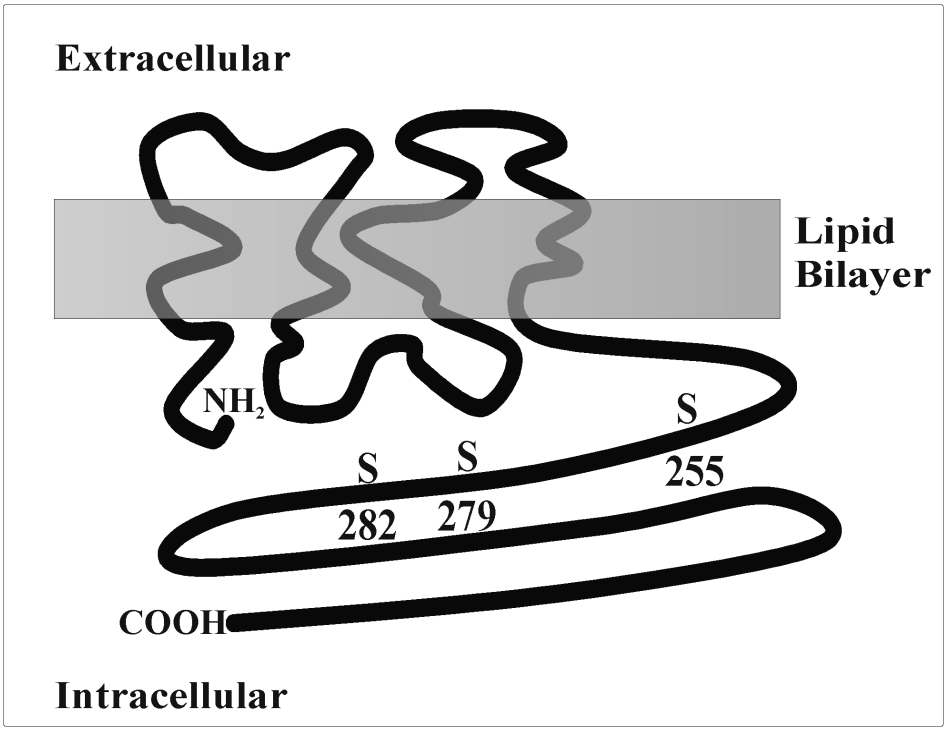

Figure 1.9. Phosphorylation sites in connexin-43

A schematic representation of rat connexin-43 as it is thought to be oriented in the plasma membrane. Three connexin-43 sites were demonstrated to be phosphorylated by ERK 1/2, Ser255 as well as Ser279/Ser282. Adapted from Lampe and Lau, 2000.

Aim

The aim of this study was to elucidate the effect of quinones with different properties on the epidermal growth factor receptor and subsequent events in WB-F344 rat liver epithelial cells. Both model (menadione, *p*-benzoquinone and 2,3-dimethoxy-1,4-naphthoquinone) and chemotherapetic quinones (doxorubicin and mitomycin C) were used in the study.

It is clinically important to understand the mechanisms through which chemotherapeutic quinones affect cellular signaling pathways. The better the mechanism of a chemotherapeutic agent is understood, the easier it might be to modulate its efficacy. Thus, the effect of various quinones on EGFR-dependent signaling cascades as well as the mechanims of action was investigated. Subsequently, the study also aimed at investigating the modulatory effect that ERK1/2 exerts on cell-cell communication through gap junctions built of connexin-43, the major connexin in the employed cell line.

2. Materials and Methods

2.1. Cell culture

WB-F344 rat liver epithelial cells were kindly provided by Dr. James E. Trosko, East Lansing, MI, USA. Cells were grown in a humidified atmosphere containing 5% (v/v) CO_2 in Dullbecco's Modified Eagle's Medium (DMEM, Sigma-Aldrich, Deisenhof, Germany), supplemented with 10% (v/v) fetal calf serum (FCS, Greiner Labortechnik, Frickenhausen, Germany), 2 mM L-glutamine (Merck, Darmstadt, Germany) and with penicillin/streptomycin (Sigma).

Treatments with DMSO (Sigma) as a control, menadione (MQ, 2-methyl-1,4-naphthoquinone, Sigma), *p*-benzoquinone (BQ, Sigma), 2,3-dimethoxy-1,4-naphthoquinone (DMNQ, Calbiochem, San Diago, CA, USA), diethyl maleate (DEM, Sigma), were usually performed in fresh serum-free medium.

The chemotherapeutic quinones, doxorubicin (Dox) and mitomycin C (MMC) were obtained from Sigma. Stock solutions (25 mM Dox and 5 mM MMC) were prepared in sterilised water that was taken as vehicle control. Cell exposure was also performed in fresh serum-free medium.

EGFR tyrosine kinase inhibitors (AG1478, Alexis Biochemicals, San Diago, CA, USA and compound 56, Calbiochem), MEK1/2 inhibitors (U0126, PD98059, Alexis Biochemicals as well as PD184352, kindly provided by Dr. Philip Cohen, University of Dundee, UK), Phosphoinositde 3-kinase (PI3K) inhibitors (wortmannin and LY 294002, Alexis Biochemicals) were applied in fresh serum-free medium 30 min prior to treatment. The NQOR-1 inhibitor, dicoumarol (ICN Biomedicals, Eschwege, Germany), was coincubated with quinones during treatments.

2.2. Toxicity assays

In this work, two methods were used to determine cell viability, based on (i) reduction of MTT (4,5-dimethylthiazol-2-yl-2,5-diphenyl-2H-tetrazolium bromide) to a colored formazan product and (ii) the uptake of a dye (neutral red) by living cells.

2.2.1. MTT-test

Cell viability can be determined using an assay based on the reduction of the yellow MTT to an insoluble purple formazan in metabolically active cells (Mosmann 1983). 5 mg MTT were dissolved in phosphate-buffered saline (PBS, 137 mM NaCl, 2.7 mM KCl, 1.4 mM KH_2PO_4 and 4.4 mM Na_2HPO_4, pH 7.5).

WB-F344 rat liver epithelial cells were cultured in 24 well plates. After incubation with DMSO or quinones, cells were washed with PBS and then kept in complete DMEM medium for 24 hours. 0.5 ml MTT (0.2 mg/ml) was added to each well after washing with PBS and incubated for 2 h at 37°C and 5% CO_2. The generated formazan was solubilized by addition of 0.5 ml SDS/HCl solution (10 % (w/v) SDS / 0.1 M HCl). Incubation overnight was preferred for complete solubilization. The cell lysates were briefly sonicated and then every sample was diluted 1:3 with PBS. The absorbance, which is proportional to cell viability, was measured at 570 nm with background subtraction at 700 nm.

The cell viability of control samples was considered 100 % from which the relative cell viability of treated samples was calculated.

2.2.2. Neutral red assay

The neutral red (NR, 3-amino-7-dimethyl-2-methylphenazine) cytotoxicity assay is based on the ability of viable cells to incorporate neutral red. NR is a weak cationic dye that readily penetrates cell membranes, accumulating intracellularly in lysosomes.

WB-F344 rat liver epithelial cells were cultured in 24 well plates. After treatments, the medium was replaced with 0.5 ml NR-containing FCS-free-medium (16.5 µg/ml), and after incubation for one hour at 37°C to allow for uptake of the dye, cells were washed twice with PBS. The dye was then extracted from the intact, viable cells with a solution of 1 % acetic acid and 50% ethanol (1 ml/well). The plates were agitated for one hour at room temperature and the absorbances were then recorded photometrically at 550 nm with background subtraction at 405 nm.

2.3. SDS-Polyacrylamide-Gel-Electrophoresis (PAGE)

For casting gels of 10 % acrylamide table 2.1 provides a guideline. The indicated volumes are sufficient for three mini gels.

Immediately after adding the ammonium persulfate (APS, 10 %) and TEMED (Sigma), the solution mixture was loaded into the gel plate sandwich to the appropriate height and enough room was left to accommodate the stacking gel. The gel solution was directly overlaid with water or iso-propanol. After polymerization (about 45 min), the overlay was removed and the surface of the gels were rinsed with MilliQ water. Directly after loading the stacking gel solution into the space above the separating gels, the sample combs were pushed down into the gel solution and the gels were left to polymerize (~30 min). Polymerized gels can be stored at 4°C wrapped in SaranWrap.

Solutions	Running gel	Stacking gel
Running gel buffer (2,5X)	16 ml	0.0
Stacking gel buffer	0.0	3 ml
Acrylamide	13.3 ml	2.5 ml
H_2O	10.6 ml	9.4 ml
TEMED	30 µl	30 µl
APS (10 %)	300 µl	300 µl

Table 1.1. Composition of buffers for the preparation of 3 mini-gels (10 %)

Running gel buffer (2,5X, pH 8.9), is composed of 3.7 M Tris and 0.25 % SDS. Stacking gel buffer (5X, pH 6.7), is composed of 0.3 M Tris and 0.5 % SDS.

To load samples for electrophoresis, the combs were carefully removed and the wells were rinsed with water to remove any unpolymerized acrylamide. The gels were then clamped onto the gel apparatus (Novex Mini-Cell, Invitrogen) that was then filled with 1x electrophoresis buffer (5X electrophoresis buffer is composed of 0.25 M Tris, 1.92 M glycin and 0.5 % SDS, pH 8.3).

Cells were lysed in sample buffer (2x SDS-PAGE Lysis (sample) buffer composed of 125 mM Tris/HCl, 4% (w/v) SDS, 20% (w/v) glycerol, 0.2% (w/v) bromophenol blue, pH 6.8 and, freshly added, 100 mM DTT).

Samples were heated in sample buffer to 95°C for 10 min before loading equal volumes to each well. Electrophoresis was performed at 40-50 milliamps of constant current per gel. After electrophoresis, the proteins on the gel were transferred into a membrane for western blot analysis (see below).

2.4. Western Blotting

Western blotting is a technique for the electrophoretic transfer of proteins to a membrane to allow probing a particular protein. This method uses an antibody to detect a specific protein from the mixture blotted to the membrane. The primary antibody sticks to the protein. A secondary antibody detected against the primary antibody and labelled with horseradish peroxidase is then hybridised.

Proteins were first separated by SDS-PAGE (see above) and the gel was removed from the electrophoresis cassette and equilibrated in transfer buffer (10X transfer buffer composed of 250 mM Tris and 2 M glycin, pH 8.3) that contained 20 % methanol.

The PVDF membrane (Amersham Biosciences, Braunschweig, Inc.) was activated by dipping it in methanol and then placed in transfer buffer containing methanol. The blotting sandwich must be arranged as shown in Figure 2.1.

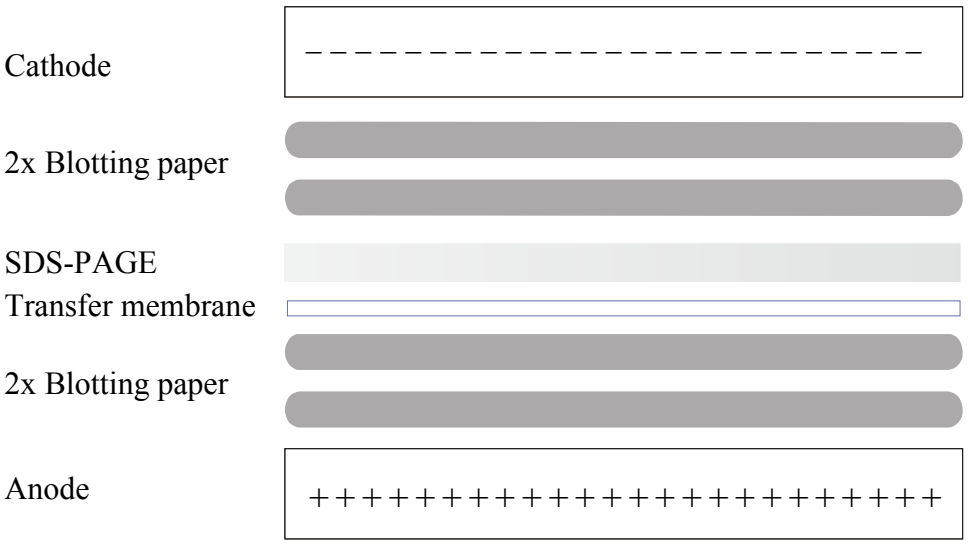

Figure 2.1. A sketch of an electrophoretic unit for western blotting

After transfer, the membrane was stained with 0.1% Ponceau S (in 5% acetic acid) for 1 min to monitor the success of the transfer process. The membranes were washed with TBST (20 mM Tris, 137 mM NaCl and 0.1% (v/v) Tween-20, pH 7.6) to remove the Ponceau S solution and then blocked for at least 60 min with 5 % non-fat dry milk powder (Bio-Rad) in TBST. If anti-connexin-43 antibody (Zymed) was used as primary antibody, blocking was performed overnight.

Immunodetections were performed employing the following primary antibodies; anti-phospho-ERK1/2 (Thr202/Tyr204), anti-total-ERK1/2, anti-phospho-ERK5, anti-phospho-Akt (Ser473), anti-total-Akt (Cell signaling Technology, Beverly, MA, USA) for 16 hr at 4 °C. Anti-connexin-43 antibody was employed for 60 min at room temperature. The membranes were washed with TBST, which was changed at least 3 times, and then incubated with the secondary antibody HRP-linked anti-rabbit, for at least 60 min at room temperature. After washing for at least 60 min, the membranes were developed by the chemiluminescence method (ECL; Amersham Biosciences, Inc. or "SuperSignal pico" substrate from Pierce/Perbio, Rockford, IL, USA). Care was taken not to allow the membranes to dry out during any of the previous steps.

The detected signals were then removed from the membrane by its incubation with stripping buffer (62.5 mM Tris, 2 % (w/v) SDS, 100 mM β-mercaptoethanol, pH 6.8) at 50°C for 30 min. The membrane was washed with de-ionized water for 10 min followed by washing with TBST, which was changed at least 3 times, for 15 min and blocking with 5 % milk powder for 60 min. The same procedures were followed, as above, but with different antibody to control the total amount of protein loaded. For example, detection of ERK1/2 phodphorylation was followed by total-ERK1/2 detection after stripping by employing anti-ERK1/2 antibody.

2.5. Dot-Blot

This method allows the detection of a particular protein in crude preparations such as cell lyaste using a specific antibody against it. Nitrocellulose membrane (BIO-RAD, Trans-Blot™ etc) was used to detect the phosphorylation of connexin-43 using SA226P, an anti-phospho-connexin-43 Ser279/Ser282, a kind gift from Dr. Kerstin Leykauf and Dr. Angel Alonso, the German Cancer Research Center, Heidelberg (Leykauf et al., 2003). On the nitrocellulose membrane a grid was drawn using a pencil to indicate the region of loading

(Figure 2.2). 2 µl of samples were slowly loaded onto the nitrocellulose membrane at the centre of the grid and air-dried. For immunodetection, the membrane was treated like those after electroblotting: blocking in 5 % milk powder in TBST for 1 h at room temperature was followed by incubation with primary antibody overnight at 4°C and secondary antibody for 1 h at room temperature. As primary antibody, a rabbit polyclonal anti-phospho-connexin-43 antibody was used. This antibody specifically recognises connexin-43 phosphorylated at Ser279 and Ser282, the sites phosphorylated by ERK 1/2. Stripping the membrane and reprobing with anti-connexin-43 antibody controlled the presence of equal amounts of connexin-43.

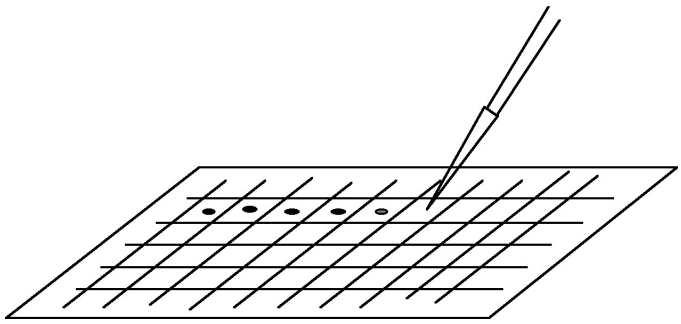

Figure 2.2. Sample loading on Dot-Blot

2.6. Immunohistochemistry

Immunohistochemistry is a technique for identifying cellular or tissue constituents (antigens) by means of antigen-antibody interactions.

WB-F344 cells were prepared on coverslips and when they reached 80-90% confluence they were washed with PBS and kept in serum-free medium overnight before treatment. After treatment, cells were washed 3 times with ice-cold PBS and fixed with methanol (5 ml per dish) for 15-20 min at -20°C. Fixed cells were then thoroughly washed with ice-cold PBS, followed by blocking with 5 % (v/v) normal goat serum (Gibco BRL, Rockville, MD, USA) in PBS containing 0.3% (v/v) Triton X-100 for 90 min at room temperature. For detection of total connexin-43 or the phosphorylated connexin-43, cells were incubated with the respective antibody at 4°C overnight under slight agitation. The rabbit polyclonal anti phospho-connexin 43 antibody (sc-12900-R, Santa Cruz, CA, USA) was diluted 1:1,500 in PBS containing 1% (v/v) goat serum. Cells were then washed with PBS and

incubated with an Alexa 488-coupled goat anti-rabbit IgG (H+L) antibody (Molecular Probes, Eugene, OR, USA) for 1 h at room temperature. Nuclear staining was performed after intense washing with PBS by addition of 4',6-diamidino-2-phenylindole (DAPI, 0.2 µg/ml final concentration) in PBS for 15 min, followed again by intense washing and embedding with Fluoromount-G (Southern Biotechnology Associates, Birmingham, AL, USA). Images were taken with a Zeiss Axiovert fluorescent microscope coupled to a CCD camera (ORCA II, Hamamatsu, Japan).

2.7. Glutathione determination

Total glutathione and glutathione disulfide were determined enzymatically according to Anderson (1985) with minor modifications. This method utilises the enzymatic recycling reaction of glutathione reductase, for the quantification of glutathione (Figure 2.3*A*). GSH reduces DTNB (also known as Ellman's reagent to produce the yellow 5-thio-2-nitrobenzoic acid (TNB) and GSSG is then recycled at the expense of NADPH with glutathione reductase. Measurement of the time dependent increase in absorbance of TNB at 412 nm provides an accurate estimation of GSH in the sample. Quantification of GSSG can be accomplished by derivatizing GSH with 2-vinylpyridine (Figure 2.3*B)*.

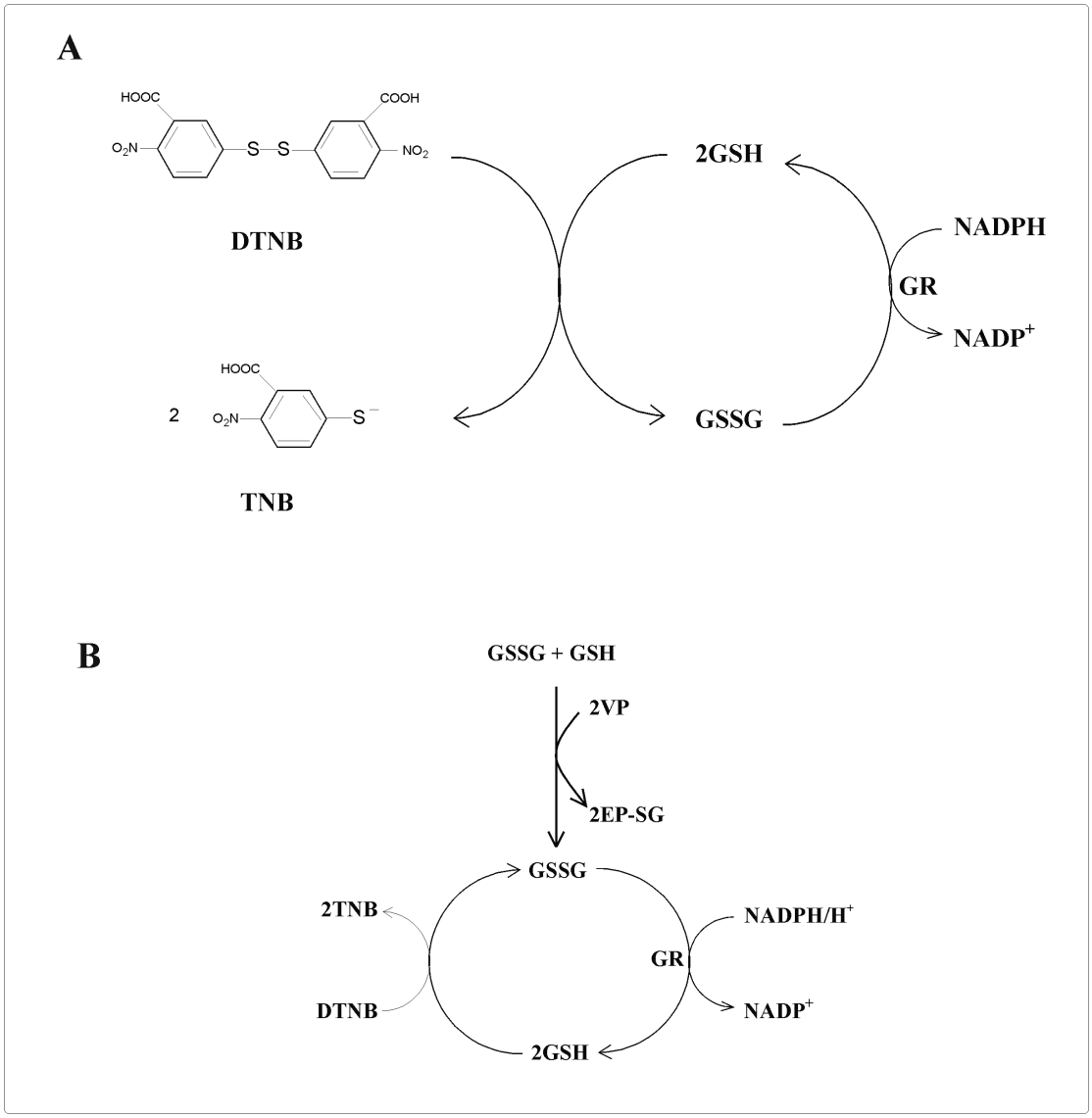

Figure 2.3. Principle of total glutathione (*A*) and glutathione disulfide (*B*) quantification (see text)

The above principles of glutathione and glutathione disulfide determination were used to determine their intracellular levels in WB-F344 cells.

Cells were cultured in 7 cm^2-cell culture dishes and after treatments they were lysed by scraping them in 250 µl of ice-cold HCl (10 mM). Cell lysates were stored at –20°C until use. Glutathione and protein standards were first prepared and measured before measuring the treated samples. One freeze/thaw cycle was followed by brief sonication of the samples on ice and centrifugation at 20,000 *g* and 4°C for 10 min to remove cell debris. Aliquots of the supernatants were kept for protein determination according to Bradford (see below). For glutathione determination, protein was precipitated from the supernatant with 5 %

(w/v; final concentration) of 5-sulfosalicylic acid (Merck) on ice. Samples were vortexed and centrifuged at 20,000 *g* and 4°C for 10 min. 900µl glutathione reaction buffer (9.42 ml of 0.2 M Phosphate buffer-0.1 mM EDTA, 0.476 ml of 10 mM DTNB (Sigma) and 100 µl of 3 mM NADPH, Sigma) were combined with 75 µl protein-free sample. 5 unit/mg Glutathione reductase (Fluka) was added at the end directly before starting the measurement at 412 nm. Care was taken in protecting DTNB from light and the glutathione reaction buffer was freshly prepared daily. 10 mM DTNB composed of 39.6 mg DTNB and 100-150 mg $NaHCO_3$ in 10 ml dH_2O.

GSSG was determined by mixing 3 µl of 2-vinylpyridine solution (Fluka) with 58 µl of 1:10 (v/v) diluted triethanolamine (Fluka) under the hood followed by addition of 100µl protein-free sample. The solution mixture was vortexed and the pH was tested using pH-paper. After 1h incubation at room temperature, GSSG measurements were performed as explained above, 900 µl reaction buffer, 75 µl sample and 25 µl glutathione reductase. Since the 2-vinylpyridine inhibits glutathione reductase to some extent, the standard was prepared in the same way.

2.8. Protein determination according to Bradford

The Bio-Rad Protein Assay, based on the method described by Marion Bradford in 1976, is a simple and accurate method for determining the concentration of solubilized protein. It was performed with the Bio-Rad Protein Determination assay according to the manufacture´s instructions.

2.9. UV spectra

Absorbance spectra were recorded on a Perkin-Elmer Lambda 2 spectrophotometer. Stock solutions of quinones (100 mM) were prepared in DMSO. A stock solution of 5 mM GSH (reduced glutathione) was prepared in PBS. In a quartz cuvette the spectra of quinones (MQ, BQ or DMNQ) were recorded. The spectra of quinone-GSH mixture were recorded after well-stirred addition of 2.5 µl quinone to 917.5 µl PBS that was finally mixed with 80 µl GSH. The final concentration of all quinones was 0.25 mM and of GSH was 0.4 mM. Spectra were recorded in the range of 200-600 nm (60 nm/min) at room temperature.

2.10. Techniques to measure gap junctional communication

Scrape-loading and microinjection were used to determine the intercellular communication of WB-F344 cells. If cells communicate, they are able to exchange ions and small molecules (≤ 1000 Dalton). Microinjection of fluorescent dyes such as Lucifer Yellow CH (MW 457.3) is a powerful tool to demonstrate the transfer of these small molecules through gap junction channels. However, another modification was made of this latter technique by scraping a monolayer of living cells in the presence of Lucifer Yellow CH, allowing the dye to spread for a fixed period. To get a reliable statistical result, microinjection is the more suitable method.

2.10.1. Scrape-loading

Scrape loading was performed as described by Sharov et al. (1999) with minor modifications. WB-F344 cells were cultured in 30 mm dishes until they reached 80-90% confluency. Cells were washed with PBS and starved overnight by keeping them in FCS-free medium. Cells were then washed with PBS and exposed to doxorubicin (100 μM) for 1h. After washing the PBS, the cell monolayer was scraped with a surgical blade followed by additional washing to remove cell debris. Cells were then incubated with Lucifer Yellow CH, Sigma, (1 mg/ml in HBSS) for 2 min followed by intensive washing for a complete removal of Lucifer Yellow. The fluorescent images were acquired directly after adding 2 ml FCS-free medium.

2.10.2. Microinjection

Cells were grown on 30 mm plastic dishes, keeping them in FCS-free medium overnight. The intracellular microinjection of the fluorescent tracer Lucifer Yellow CH [10% (w/v) in 0.33 M LiCl] was performed as described (Klotz et al., 2002b). A thin tip (Femtotip) was filled with Lucifer Yellow CH solution and transferred into borosilicate glass capillaries. After the respective treatment, cells were washed with PBS, 2 ml FCS-free medium and Lucifer Yellow CH was injected into selected cells with a micromanipulator and a microinjector system. The number of fluorescent cells surrounding the loaded cells was counted 20 seconds after injection. 10 individual cells per dish were loaded with dye, and means of the numbers of fluorescent neighboring cells were calculated.

2.11. Statistics and imaging

Data are expressed as means ± S.D. Comparisons between groups were done with one-way analysis of variance followed by Student-Newman-Keuls test. A p value of less than 0.05 was considered significant. For Western blotting or dot blotting the presented results are representative for at least 3 independent experiments. Densitometric analyses were performed using Scion Image software (Scion Corporation, Frederick, MD).

3. Results

3.1. Cytotoxicity of Quinones (Menadione, *p*-Benzoquinone and DMNQ)

The cytotoxicities of menadione (MQ), *p*-benzoquinone (BQ) and 2,3-dimethoxy-1,4-naphthoquinone (DMNQ) in WB-F344 cells were evaluated using the MTT assay. The toxic effect of all quinones increased in a time and concentration dependent manner (Figure 3.1). Cells were cultured in 24-well plates, exposed to gradually increased concentrations of MQ, BQ or DMNQ for 15, 30 or 60 min, followed by washing with PBS and incubation with normal DMEM complete medium for 24 h. Thereafter, the MTT assay was performed as described in Materials and Methods. Menadione was observed to be more toxic than BQ or DMNQ, with an exposure for just 15 min (50 and 75 μM) significantly decreasing 24 h survival. BQ and DMNQ also markedly affected the cells, especially after an exposure for 1h.

An MTT-test was also performed directly after treatments with quinones (Figure 3.2) to select suitable time points and concentrations for further experimental analysis. Again, menadione was observed to be more toxic than BQ or DMNQ with an exposure for 30 or 60 min (50 and 75 and 100 μM). Therefore, the time point of 15 min (no detectable toxicity) was selected with 50 μM MQ, 100 μM BQ and 100 μM DMNQ, unless noted otherwise, for investigations such as Western blot analysis and glutathione measurements (see below).

The appearance of treated cells was microscopically examined after treatment with quinones. As seen in Figure 3.3, a dramatic change in nuclear morphology was observed with menadione within 1h of exposure.

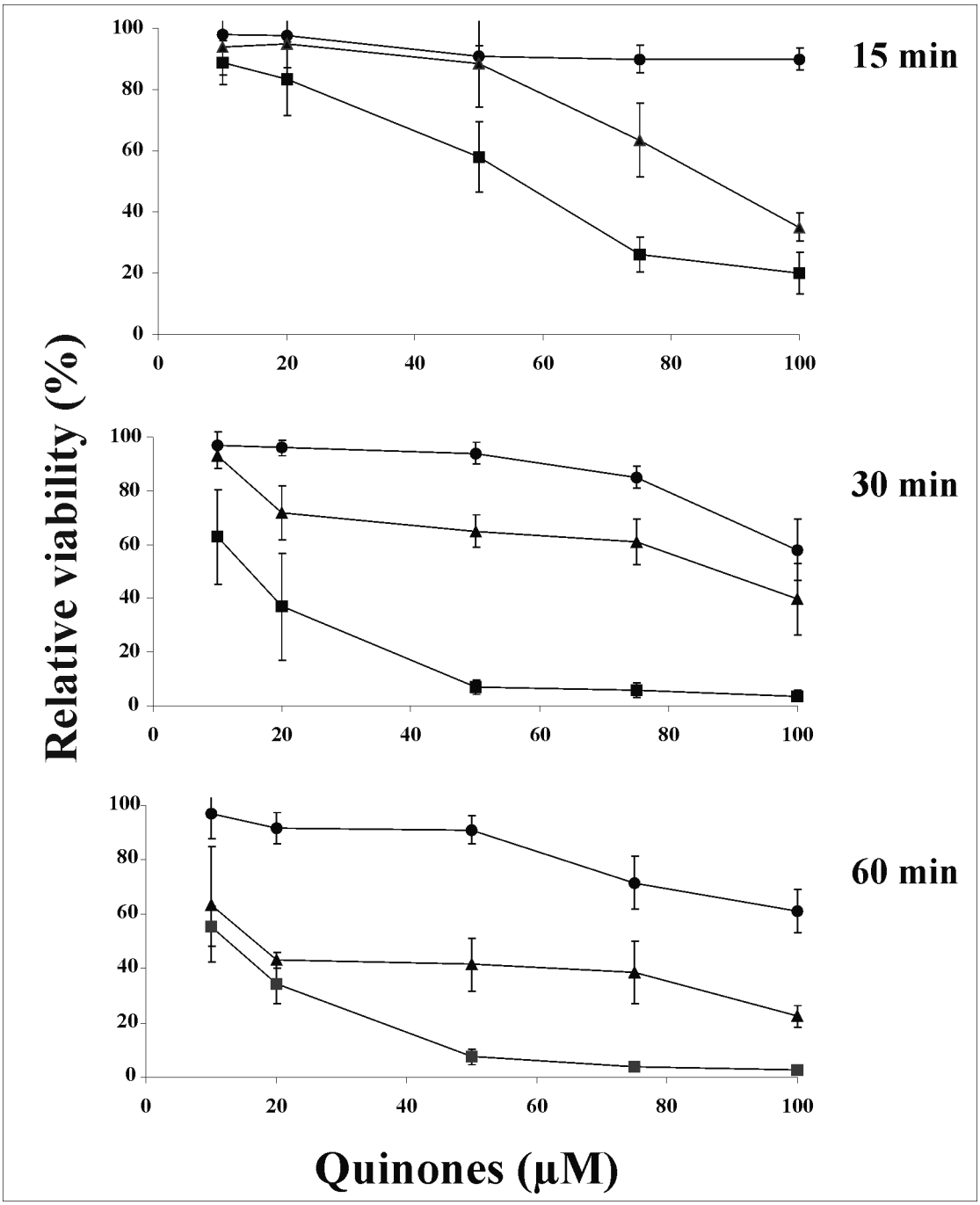

Figure 3.1. Quinone cytotoxicity (24 h after exposure)

Time course and concentration dependence for the cytotoxic effect induced by MQ (■), BQ (●) or DMNQ (●). WB-F344 cells were exposed to the indicated concentration of the respective quinone for 15, 30 or 60 min. Cells were then washed once with PBS followed by incubation with complete DMEM for 24. DMSO was taken as vehicle control. Data are means of 3 independent experiments ± SD.

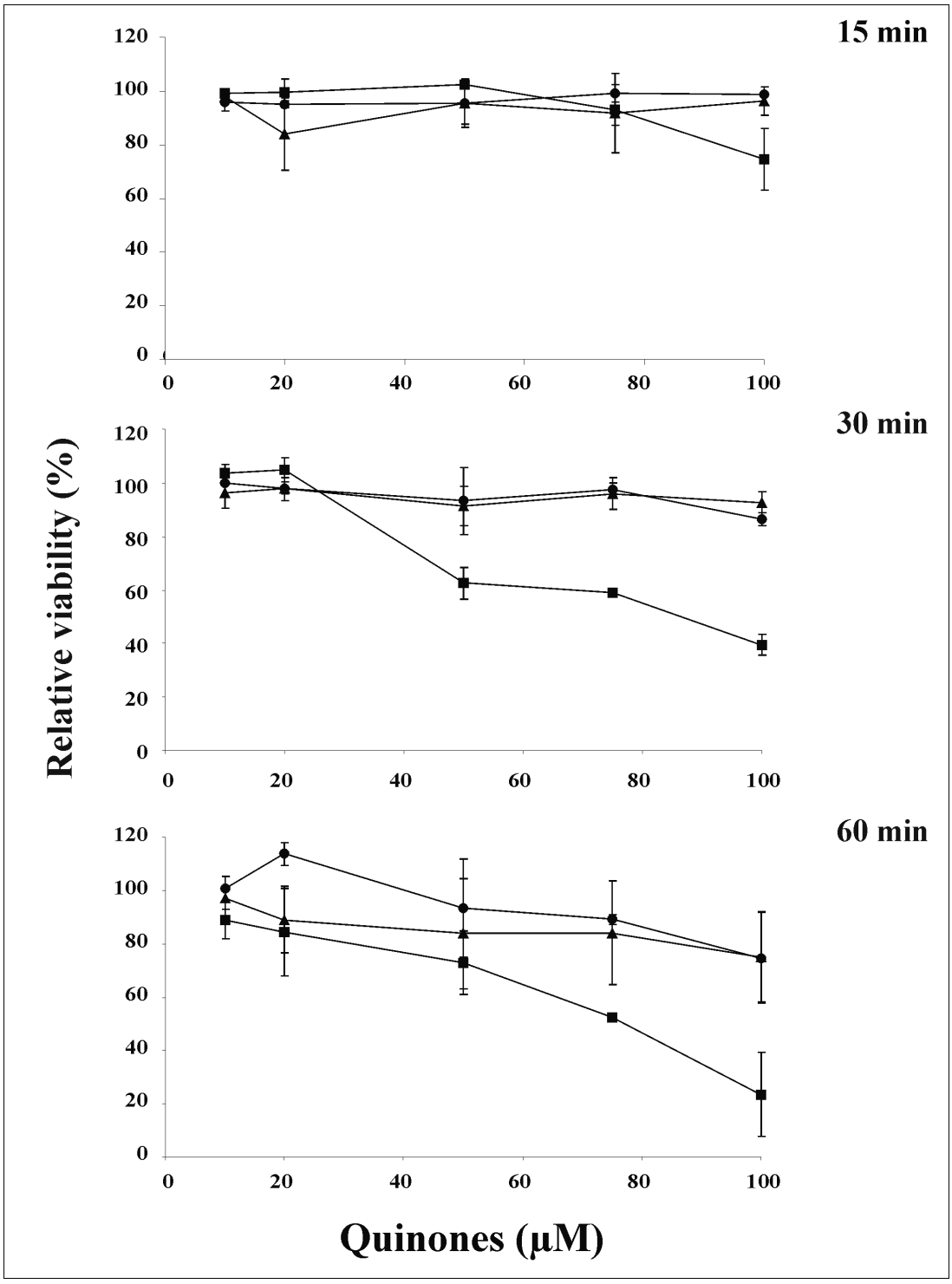

Figure 3.2. Quinone cytotoxicity (directly after exposure)

Time course and concentration dependence for the cytotoxic effect induced by MQ (■), BQ (●) or DMNQ (●). WB-F344 cells were exposed to the indicated concentrations of the respective quinone for 15, 30 or 60 min. Cells were then washed once with PBS followed by MTT measurements. DMSO was taken as vehicle control. Data are means of 3 independent experiments ± SD.

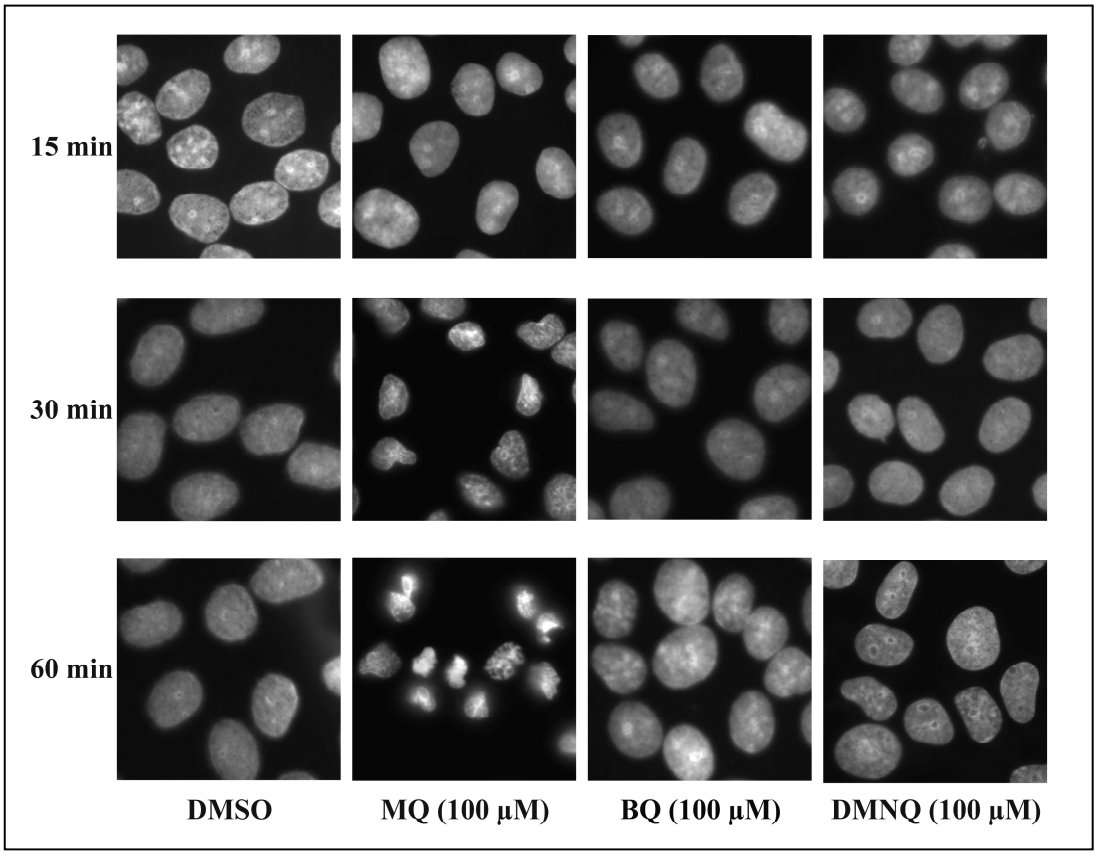

Figure 3.3. Photomicrographs of stained WB-F344 nuclei after treatment with or without quinones

WB-F344 rat liver epithelial cells were exposed to DMSO (control), MQ, BQ, or DMNQ (100 µM each) for 15, 30 or 60 min, followed by washing with ice-cold PBS and DAPI staining as explained in Materials and Methods.

3.2. Activation of ERK 1/2 after exposure to quinones

Exposure of cells to menadione is known to result in the activation of the extracellular signal-regulated kinases ERK1 and ERK2 (Klotz et al, 2002b). Two other quinones of different reactivities were tested for ERK activation: *p*-benzoquinone (BQ), a strong alkylator, and 2,3-dimethoxy-1,4-naphthoquinone (DMNQ), an exclusive redox cycler, and compared with menadione, which is known both to undergo redox cycling and to alkylate.

Exposure of WB-F344 cells to any of the three quinones resulted in the strong dual phosphorylation of ERK1/2 (Figure 3.4). Cell exposure to all quinones was performed in fresh FCS-free medium followed by Western blotting as described in Materials and Methods.

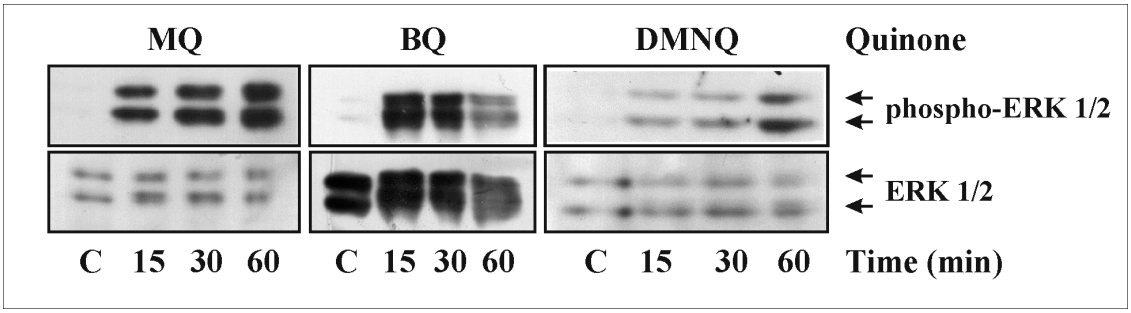

Figure 3.4. ERK activation by quinones

WB-F344 rat liver epithelial cells were exposed to menadione (MQ, 50 µM), *p*-benzoquinone (BQ, 100 µM) or 2,3-dimethoxy-1,4-naphthoquinone (DMNQ, 100 µM) for the times indicated, followed by determination of ERK1/2 phosphorylation and total ERK1/2 levels by Western blotting.

3.3. ERK1/2 remain active after replacing quinone-containg media with serum free medium

When cells were exposed to any of the quinones for 15 min, followed by aspiration of quinone-containing media and postincubation in serum-free medium, activation of ERK 1/2 remained equally strong, with slight decreases observable starting after 2h of postincubation (Figure 3.5). This might indicate that the metabolites of these quinones such as hydroquinones or H_2O_2 from redox cycling (Figure 1.3) are produced for at least 2 h after removal of the quinone. It might also mean that an initial modification of a signaling protein, leading to ERK1/2 activation, needs at least 2 h to be repaired by reversal of the modification protein or substitution of the protein.

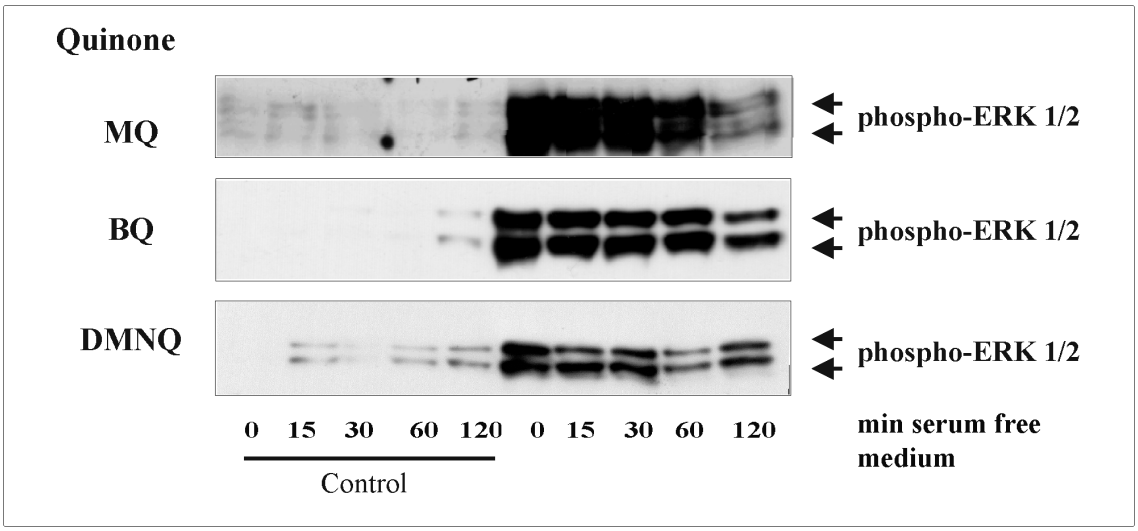

Figure 3.5. ERK1/2 remain active after aspiration of the quinones-containing media
WB-F344 rat liver epithelial cells were exposed to DMSO (control) or menadione (MQ, 50 µM), BQ (100 µM) or DMNQ (100 µM) for 15 min, followed by aspiration of the quinones-containing media, washing with PBS and adding serum free medium for the time indicated. After each time point ERK1/2 phosphorylation was determined by Western blotting.

3.4. Quinone-induced ERK1/2 activation is mediated by MEK1/2

MAPK/ERK kinases (MEK) 1/2 are dual specificity kinases phosphorylating and activating ERK1/2. In order to delineate the role of MEK1/2 in ERK1/2 activation, a specific inhibitor of MEK activation by upstream kinases, U0126, was used.

Cells were preincubated with 10 µM U0126 or DMSO (vehicle control) in serum free medium for 30 min, followed by aspiration, washing with PBS and exposure to quinones (50 µM MQ, 100 µM BQ or 100 µM DMNQ) in the continued presence of U0126 for 15 min. Quinone-induced ERK activation was found to be mediated by MAPK/ERK kinase (MEK) 1 and MEK 2 as U0126 completely (BQ, DMNQ) or largely (menadione) blocked ERK phosphorylation (Figure 3.6).

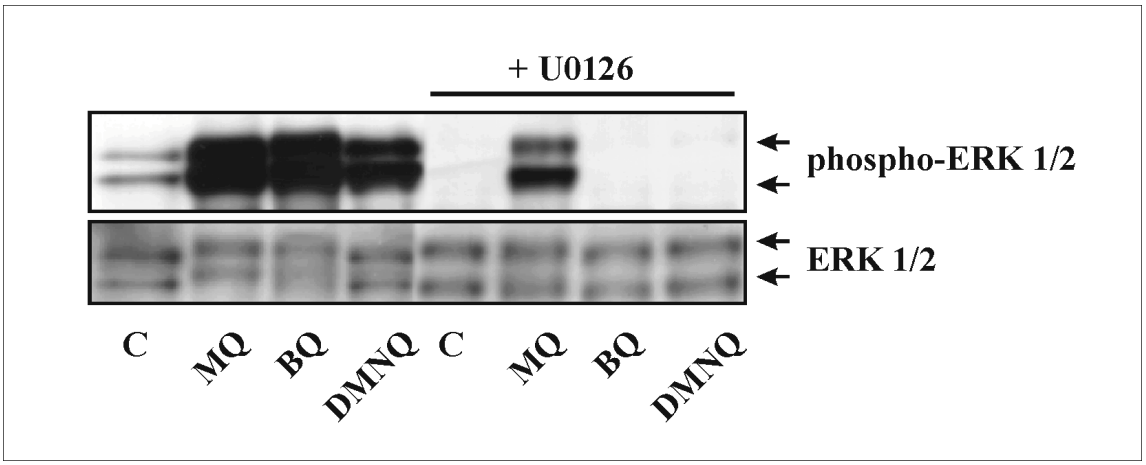

Figure 3.6. Quinones induced ERK1/2 activation is mediated by MEK1/2

WB-F344 rat liver epithelial cells were exposed to the MEK inhibitor U0126 (10 μM) for 30 min followed by washing with PBS and exposing to MQ (50 μM) BQ (100 μM) or DMNQ (100 μM) for 15 min. Thereafter ERK1/2 phosphorylation and total ERK levels were determined by Western blotting. DMSO was taken as vehicle control for the quinones ("C") and for U0126.

3.5. Role of the epidermal growth factor-receptor in quinone-induced signaling

Based on inhibitor studies, it was known that menadione-induced activation of ERK1/2 is mediated by activation of the EGFR (Klotz et al, 2002b). Indeed, as demonstrated in Figure 3.7.*A*, AG1478 and compound56, two specific inhibitors of the EGFR tyrosine kinase, largely blocked menadione-induced ERK1/2 activation. As with menadione, BQ and DMNQ-induced ERK1/2 activation relies on EGFR activation, as demonstrated using AG1478 and compound 56 (Figure 3.7*B*), both of which abrogated ERK1/2 phosphorylation induced by exposure of cells to these quinones.

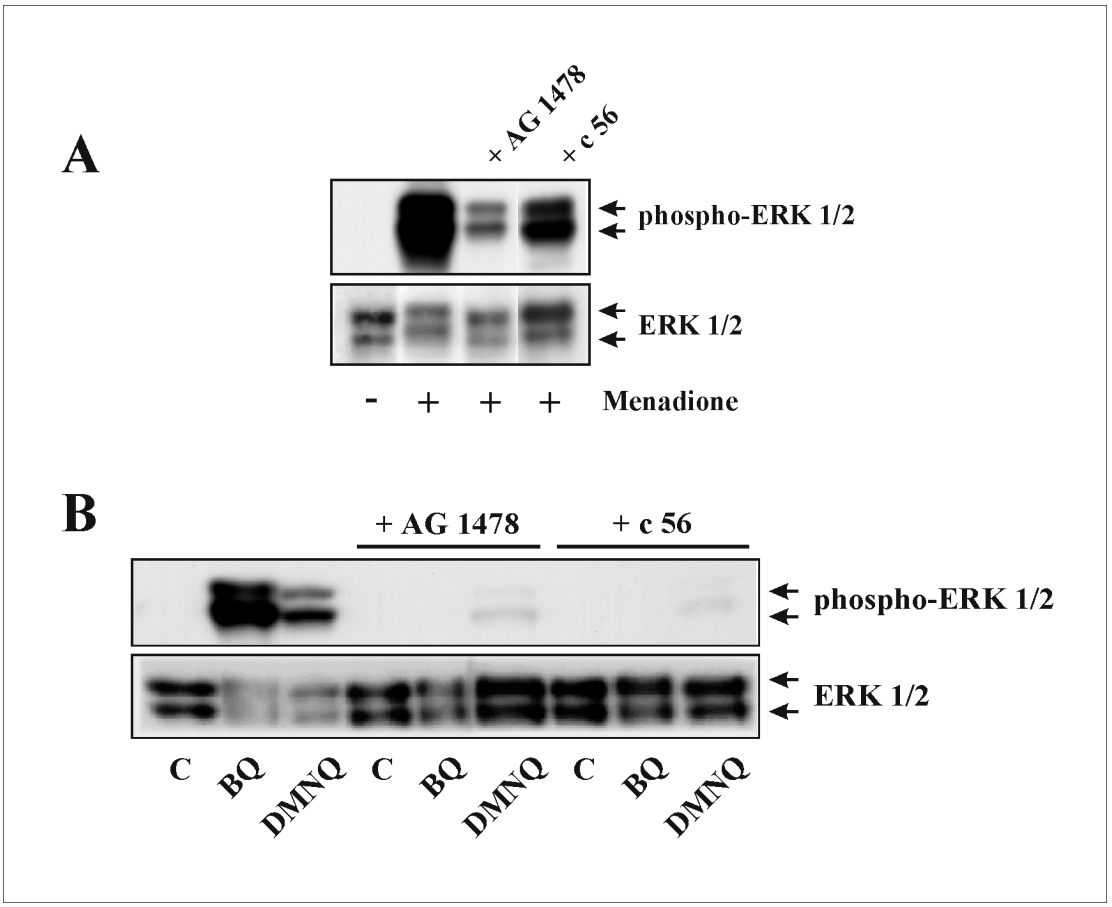

Figure 3.7. Role of EGFR in quinnone-induced ERK activation

(A) WB-F344 cells were exposed to MQ (50 µM) for 15 min with or without pre- and coincubation with inhibitors of the EGFR tyrosine kinase (AG1478 and compound 56, c56; 10 µM each), followed by analysis of ERK1/2 phosphorylation by Western blotting.

(B) WB-F344 cells were exposed to DMSO (vehicle control, "C"), BQ, (50 µM) or DMNQ (100 µM) for 30 min with or without pre- and coincubation with inhibitors of the EGFR tyrosine kinase (AG1478 and compound56, c56; 10 µM each), followed by analysis of ERK1/2 phosphorylation by Western blotting. Exposure to inhibitors alone (not shown) did not yield results different from control. DMSO served as vehicle control both for menadione and for the inhibitors.

3.6. PI3K/Akt is another EGFR-dependent pathway activated by quinones

If the EGFR is activated in cells exposed to MQ, BQ or DMNQ, as shown above, downstream signaling pathways other than the MEK/ERK pathway should also be stimulated. In fact, the phosphoinositide 3-kinase (PI3K)/Akt cascade was activated in WB-F344 cells as serine-473 phosphorylation of Akt was strongly enhanced after treatment with MQ, BQ or DMNQ, and abrogated in the presence of either of two

structurally unrelated inhibitors of PI3K, wortmannin or LY294002 (Figure 3.8). Taken together, MQ, BQ and DMNQ all activate the EGFR as well as downstream signaling pathways.

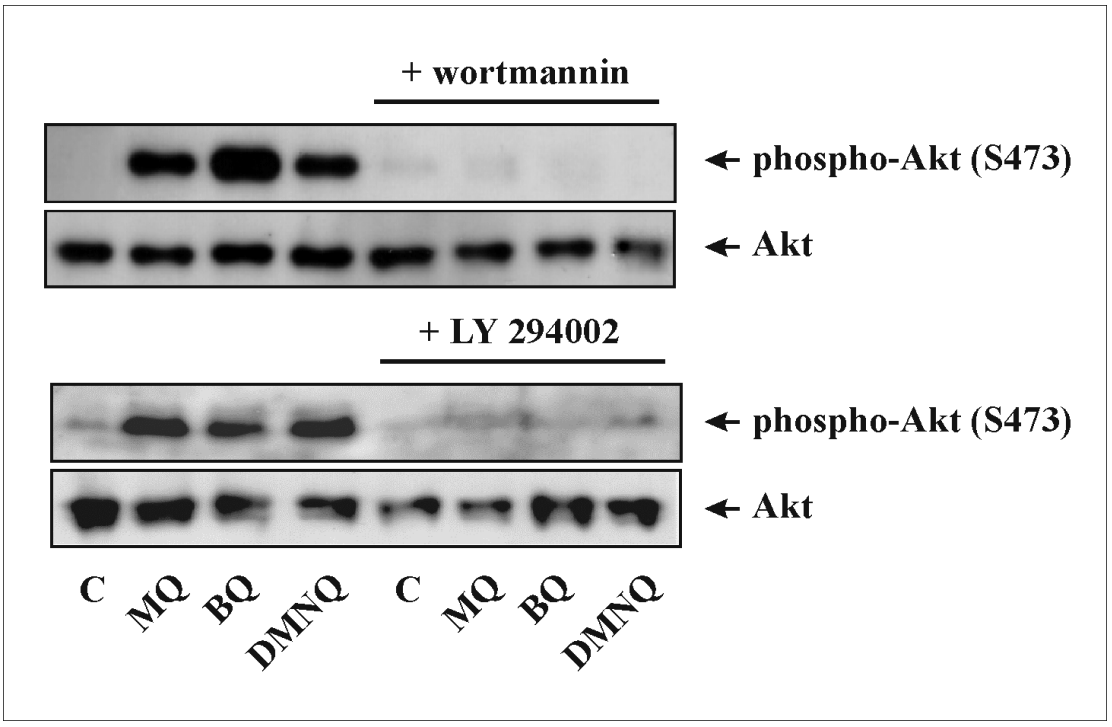

Figure 3.8. Quinones activated PI3K/Akt pathway

Cells were exposed to menadione (MQ, 50 µM), BQ or DMNQ (100 µM each) in the absence or presence of inhibitors of phosphoinositide 3-kinase, wortmannin (100 nM) or LY294002 (20 µM, lower panel). Phosphorylation at Ser473 was detected by Western blotting.

3.7. Quinone-induced ERK 1/2 activation leads to connexin-43 phosphorylation

Exposure of WB-F344 cells to menadione is known to result in the activation of ERK 1/2 and ERK-dependent phosphorylation of connexin-43, resulting in a decreased intercellular communication (Klotz et al, 2002b). The two other quinones were also tested for their ability to phosphorylate connexin-43 as they both strongly activate ERK1/2 (Figure 3.7*B*). As was demonstrated for menadione, phosphorylation of connexin-43 at Ser279 and Ser282, sites specifically recognized by ERK 1/2 (Lampe et al, 2000) was also induced in cells exposed to BQ or DMNQ (Figure 3.9). Phosphorylation of connexin-43 at ERK1/2 sites was demonstrated by both dot blotting (Figure 3.9*A*) and by immunohistochemistry (Figure 3.8*B*) using two

different polyclonal phospho-specific antibodies. As shown in Figure 3.9, all quinones stongly induced connexin-43 phosphorylation.

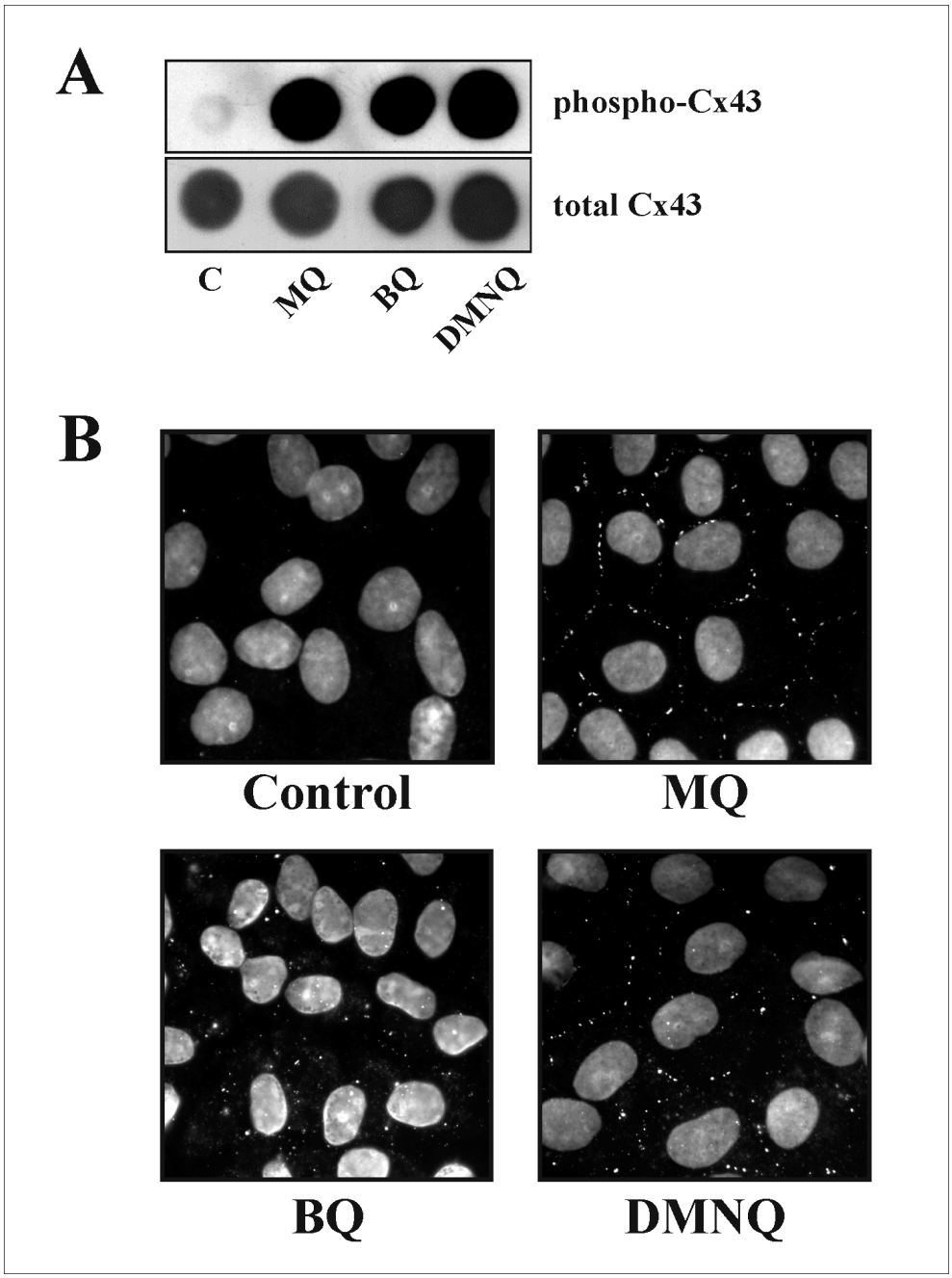

Figure 3.9. Induction of connexin-43 phosphorylation by quinones

WB-F344 rat liver epithelial cells were exposed to DMSO (vehicle control, "C"), MQ (50 μM), BQ (50 μM) or DMNQ (100 μM) for 30 min. Phosphorylation of connexin-43 at Ser279 and Ser282 was then analyzed by (A) dot blotting and (B) immunohistochemistry. In (A), loading control was by detection of total connexin-43, in (B), nuclei were stained with DAPI for orientation.

3.8. ERK activation by menadione is attributable to arylation reactions

Menadione may react intracellularly in two ways (Figure 3.10*A*), *i.e.,* by arylating nucleophilic compounds such as thiols, or by undergoing redox cycling. The latter may be expedited by NADPH-quinone oxidoreductase-1 (NQOR-1), also known as DT-diaphorase, which reduces menadione and other quinones to the corresponding hydroquinone at the expense of NAD(P)H. The hydroquinone, in turn, may be oxidized by molecular oxygen present in high micromolar concentrations in biological systems, thus generating superoxide and other reactive oxygen species derived from it. BQ is known to be a very strongly arylating quinone, whereas DMNQ is an exclusive redox cycler. To test for the involvement of redox cycling in activation of ERK1/2 by menadione, WB-F344 cells were exposed to menadione in the presence of dicoumarol, an inhibitor of NQOR. As controls, the other quinones were also examined for their capability of activating ERKs and for inhibition of the respective effects by dicoumarol. Attenuation of redox cycling by blockade of NQOR should therefore inhibit effects of DMNQ but not BQ.

Cells were coincubated with all quinones for 1 h in the presence or absence of dicoumarol (100 μM). As shown in Figure 3.10*B*, dicoumarol indeed completely blocked the effect of DMNQ only and had no effect on the arylating quinone, BQ. Activation of ERK1/2 by menadione was not impaired by dicoumarol, suggesting that ERK1/2 is largely due to the arylating effects of menadione.

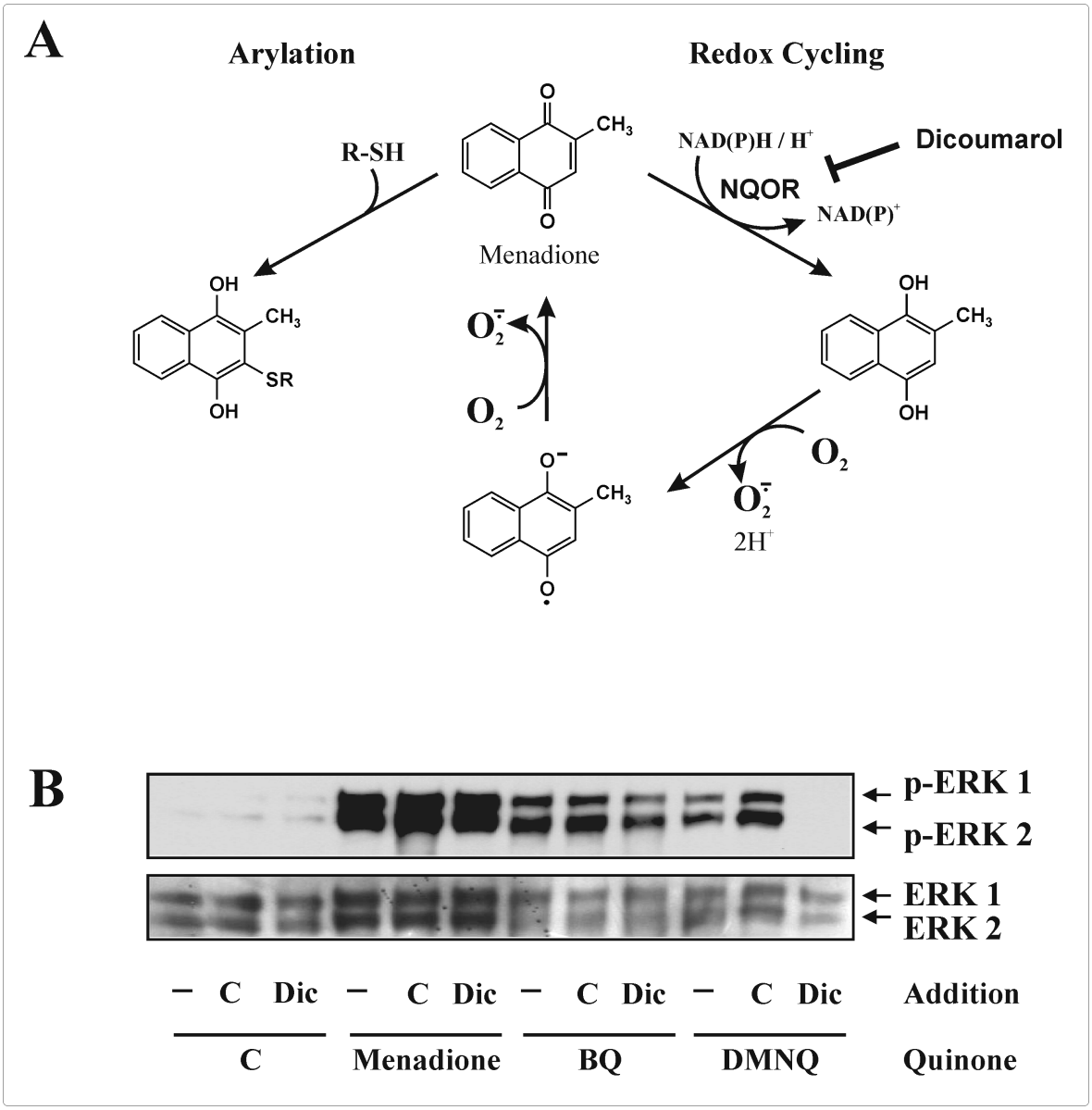

Figure 3.10. Menadione action: arylation *versus* redox cycling

(A) Scheme depicting the two major reaction pathways of menadione in mammalian cells and the role of NQOR.

(B) WB-F344 cells were exposed to 50 µM MQ, 100 µM BQ, 100 µM DMNQ, or vehicle (DMSO, *C*) in absence or presence of the NQOR-1 inhibitor dicoumarol (*Dic*, 100 µM) or additional vehicle (DMSO, *C*) for 60 min. Cells were lysed, and ERK1/2 phosphorylation was analyzed by Western blotting. A pan-ERK antibody was used to control for the presence of total ERK.

3.9. The role of glutathione in quinone-induced ERK activation

As mentioned above, the effect of quinones in the cell is due to arylation in the case of BQ, redox cycling in the case of DMNQ, or both in the case of MQ. What is arylated by MQ or BQ in the cell?

UV/Vis-spectrophotometrical analysis of solutions of quinones and/or glutathione was performed.

Menadione was found to interact with GSH, as can be seen from the difference in UV-visible spectra of menadione before and after reaction with GSH: the calculated sum spectrum of GSH plus menadione significantly differs from the spectrum measured after mixing the two compounds (Figure 3.11*A*, top). Even more dramatic spectral changes were observed with BQ (Figure 3.11*A*, middle), whereas no difference between calculated and measured spectra was seen for DMNQ (Figure 3.11*A*, bottom). This is in line (i) with BQ being a strong alkylator which is known to easily react with GSH, not only forming monoglutathionylated hydroquinone, but also di-, tri- and tetra-(glutathionyl)-hydroquinone in cells (Lau et al, 1988, and Boatman, 2000), and (ii) with DMNQ being a non-alkylating quinone: both the C2 and C3 positions are occupied.

In accordance with the spectra in Figure 3.11*A*, about 35% of the cellular GSH were depleted in cells exposed to menadione after 15 min, about 90% were lost after exposure to BQ and no more than a tendency toward GSH depletion was observed with DMNQ (Figure 3.11*B* top). Significant accumulation of glutathione disulfide was found only in cells exposed to menadione and a tendency to accumulate GSSG was seen with DMNQ (Figure 3.11*B* middle). The MQ-induced accumulation of GSSG was significantly attenuated in the presence of dicoumarol (100μM) that was used to block the redox cycling process through inhibition of NQOR-1 (Figure 3.11*B* bottom). This indicates that MQ indeed undergoes redox cycling, which, however, is not responsible for ERK activation.

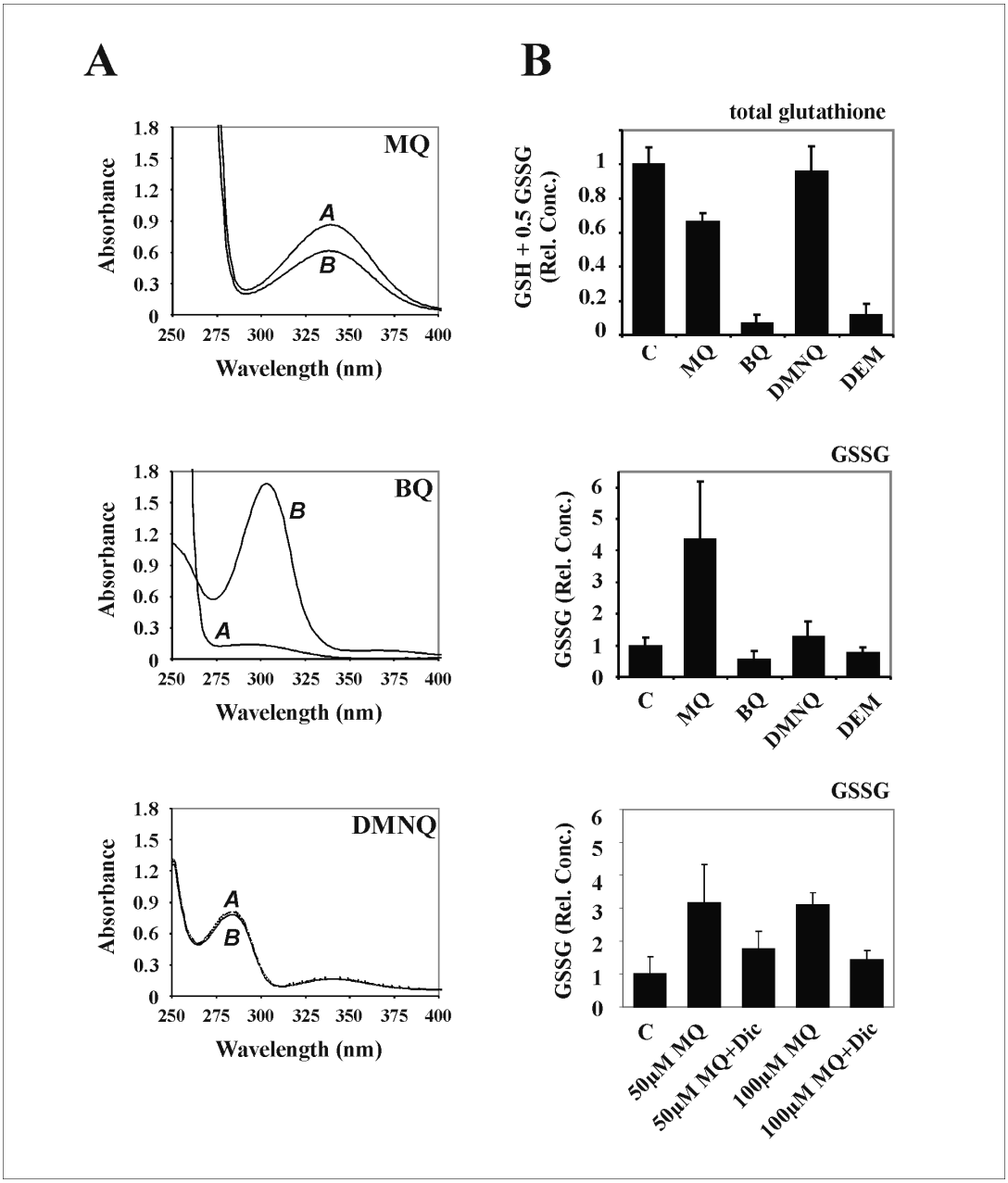

Figure 3.11. Interaction of quinones with glutathione

(A) UV/Vis spectra of a mixture of GSH (0.4 mM) with MQ, BQ or DMNQ. The final concentration of all quinones was 0.25 mM. "*A*" represent calculated sum spectra of the GSH spectra plus the quinone spectra and are expected if no interaction between GSH and quinone occurs, "*B*" are the measured spectra of GSH plus quinone mixtures. Similar spectra were observed with N-acetyl cysteine (NAC).

(B) Relative changes in total glutathione (GSH + 0.5 GSSG; top) and GSSG in the absence (middle) or presence (bottom) of dicoumarol in rat liver epithelial cells exposed for 15 min to DMSO (as vehicle control, "C"), menadione (50 µM), *p*-benzoquinone (BQ, 100 µM), 2,3-dimethoxy-1,4-naphthoquinone (DMNQ, 100 µM) or diethyl maleate (DEM, 1 mM). Data are means of at least 3 independent experiments performed in triplicate ± S.D.

In order to delineate the role of GSH depletion in activation of ERK 1/2 by quinones, cells were exposed to N-acetyl cysteine (NAC), a cell-permeant thiol employed to deliver antioxidant capacity to cells that serves as a precursor of cysteine which is utilized for GSH synthesis.

ERK1/2 activation by menadione and BQ, but not by DMNQ, was prevented by the concomitant presence of NAC with the quinones (Figure 3.12*A*). This was probably due to the direct interaction of NAC, which was applied in a 300-600-fold molar excess, with menadione or BQ, respectively. No such interaction with the non-alkylating DMNQ is to be expected. Indeed, spectral changes of the quinones in the presence of NAC were very similar to those observed with GSH in Figure 3.11.*A* (not shown).

If, however, cells were pretreated with NAC for 1-3 hours and then washed with PBS before exposure to the quinones, both BQ and DMNQ did not activate ERK 1/2 anymore, whereas menadione-induced ERK activation was unimpaired (Figure 3.12*B*). Consistent with these data, ERK activation induced by any of the quinones was significantly attenuated, if preincubation of NAC was followed by coincubation of quinones with NAC (Figure 3.12*C*). The mechanism of menadione-induced ERK activation thus obviously differs from the path taken by BQ and DMNQ.

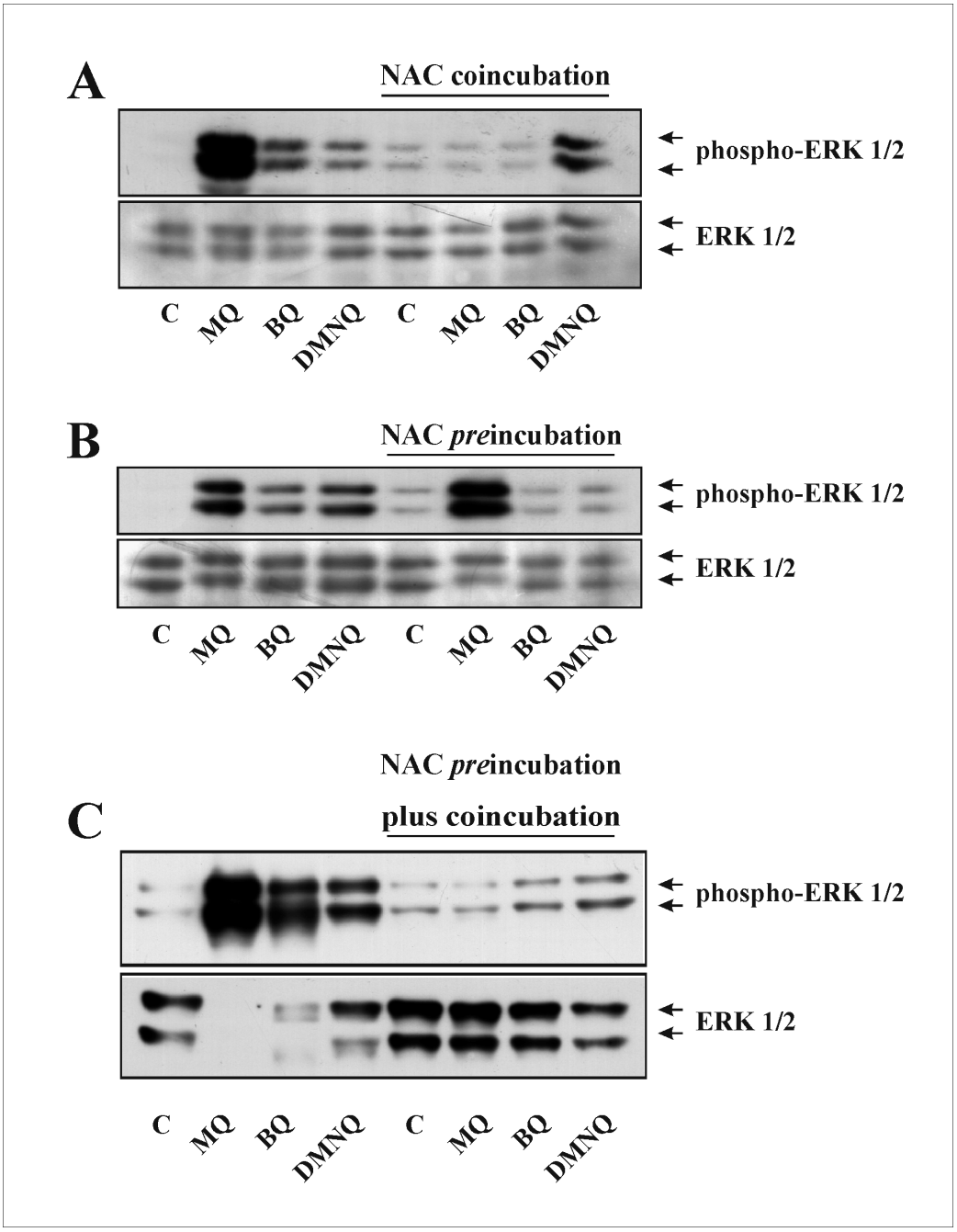

Figure 3.12. Effect of N-acetyl cysteine (NAC) on quinone-induced ERK activation

(A) Rat liver epithelial cells were exposed to menadione (50 µM), BQ (100 µM) or DMNQ (100 µM) in the presence or absence of 30 mM NAC for 15 min, followed by lysis and analysis of ERK phosphorylation and total ERK levels by Western blotting.

(B) Cells were incubated with or without NAC (30 mM) for 3h, followed by washing and exposure to the quinones or DMSO for 15 min, followed by Western blotting as in A.

(C) Cells were incubated with or without NAC (30 mM) for 3h, followed by washing and exposure to quinones or DMSO in presence or absence of NAC (30 mM) for 15 min, followed by Western blotting as in A.

3.10. Glutathione depletion leads to activation of EGFR-dependent signaling

In order to test whether the depletion of GSH might cause the activation of EGFR-dependent signaling, cells were exposed to diethyl maleate (DEM), a glutathione S-transferase substrate that is coupled to GSH, thus depleting the thiol.

Exposure of WB-F344 cells to various concentrations of DEM resulted in a concentration-dependent activation of ERK 1/2 and of Akt (Figure 3.13*A*). Eighty-three percent (83 ± 3 %, means ± SD, n = 3) of cellular glutathione was depleted with 1 mM DEM under these conditions. Interestingly, GSH depletion had to be rapid, i.e. within minutes (as with BQ), to result in the activation of ERK. Exposure of cells to buthionine sulfoximine (4 mM), an inhibitor of GSH biosynthesis, for 24 h slowly decreased total glutathione by 71 ± 9% (means ± SD , n = 3) of control, but no ERK activation was seen (data not shown).

ERK and Akt activation was blocked in the presence of inhibitors of the EGFR, AG1478 and compound56. Interestingly, this activation was also partly prevented by AG1295, an inhibitor of the PDGF receptor tyrosine kinase (Figure 3.13*B*), pointing to a minor role of another receptor tyrosine kinase in addition to EGFR.

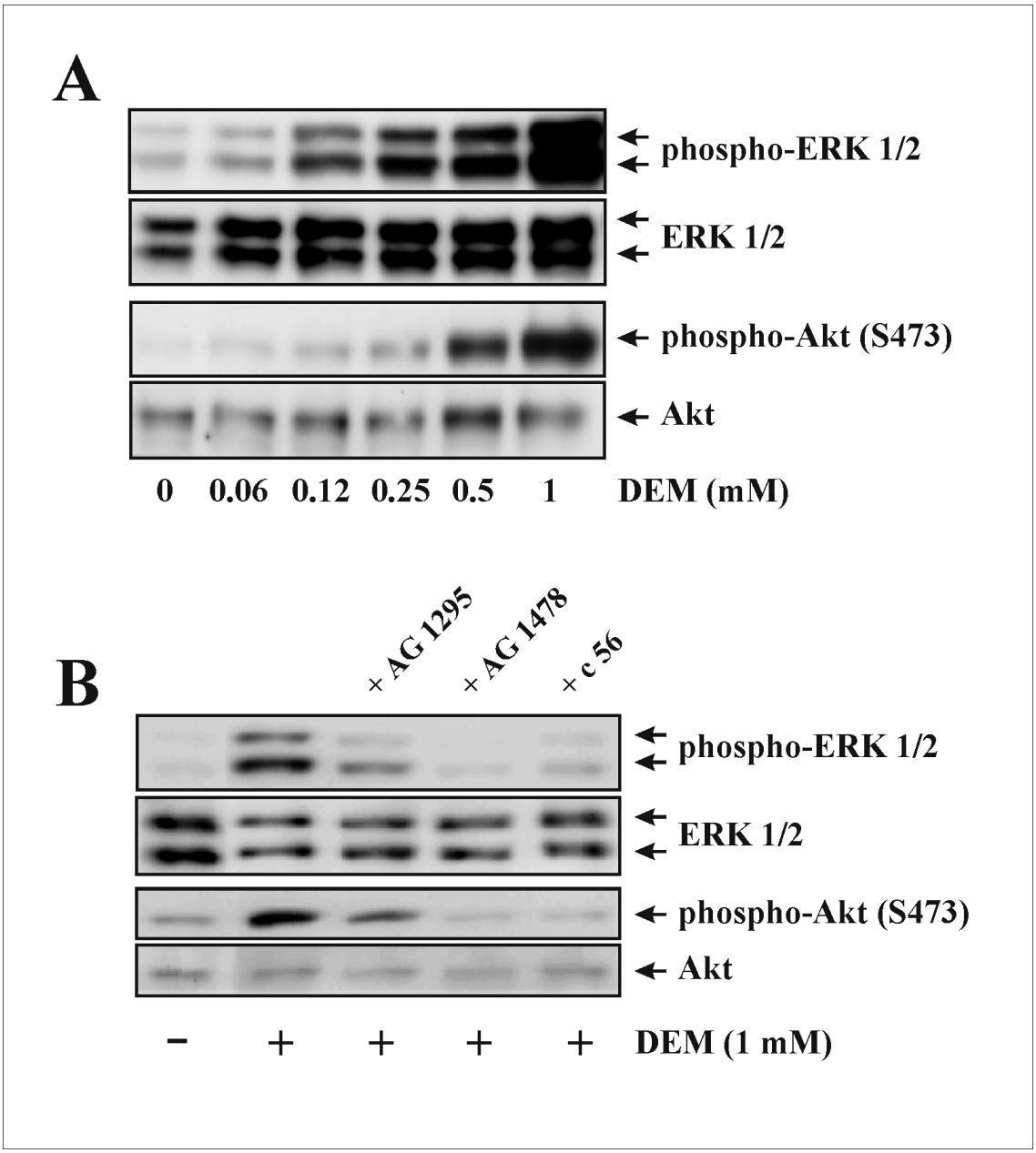

Figure 3.13. ERK activation induced by GSH depletion

(A) Rat liver epithelial cells were exposed to diethyl maleate at the indicated concentrations for 60 min, followed by lysis and analysis of ERK and Akt phosphorylation and total ERK/Akt levels by Western blotting.

(B) Inhibitors of PDGF receptor (AG1295, 10 µM) or EGFR (AG1478, compound56, c56, both 10 µM) were added to the cells 30 min prior to DEM. DMSO served as vehicle control both for DEM and for the inhibitors. Exposure to inhibitors alone (not shown) did not yield results different from control.

3.11. ERK activation induced by GSH depletion leads to phosphorylation of connexin-43

As with menadione or BQ, the depletion of GSH by application of DEM entails phosphorylation of the ERK 1/2-specific sites of Cx43, Ser279 and Ser282, as demonstrated by dot blotting (Figure 3.14*A*) and immunocytochemistry (Figure 3.14*B*) using two different antibodies.

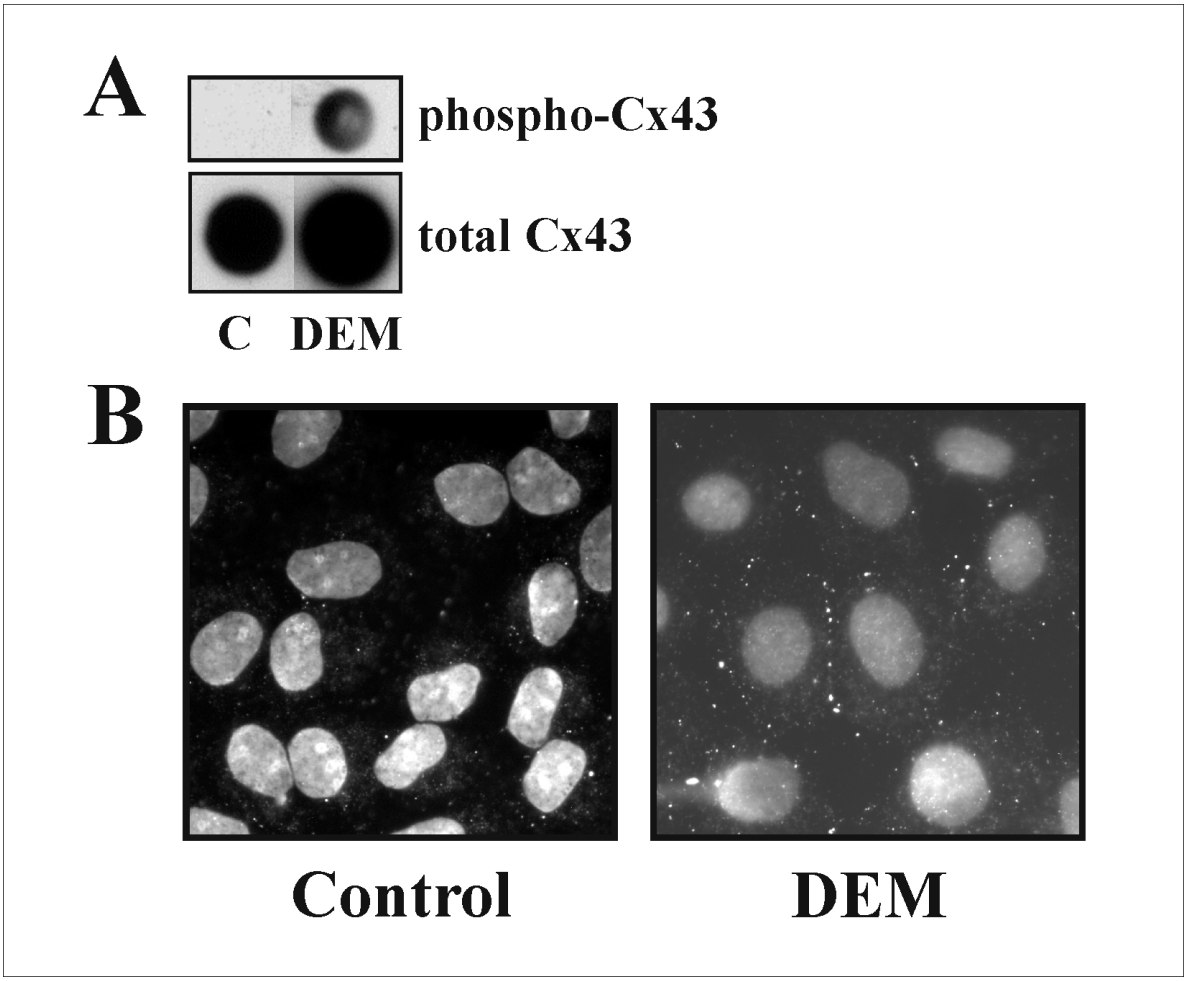

Figure 3.14. Induction of connexin-43 phosphorylation by glutathione depletion

WB-F344 rat liver epithelial cells were exposed to DMSO (vehicle control, "C") or diethyl maleate (DEM, 2 mM) for 30 min. Phosphorylation of connexin-43 at Ser279 and Ser282 was then analysed by (A) dot blotting and (B) immunohistochemistry. In (A), presence of equal amounts of connexin was tested for by detection of total connexin-43; in (B) nuclei were stained with DAPI for orientation.

3.12. Cytotoxicity of chemotherapeutic quinones (doxorubicin and mitomycin C)

The cytotoxicity of both doxorubicin (Dox) and mitomycin C (MMC) was compared and evaluated by MTT assay. Cells were cultured in 24-well plates, exposed to 100 µM Dox or MMC for 30 and 60 or 120 min, followed by washing and incubation with normal DMEM for 24 h. Thereafter, an MTT assay was performed as described in Materials and Methods (Figure 3.15). At the indicated concentrations, doxorubicin is much more toxic than MMC.

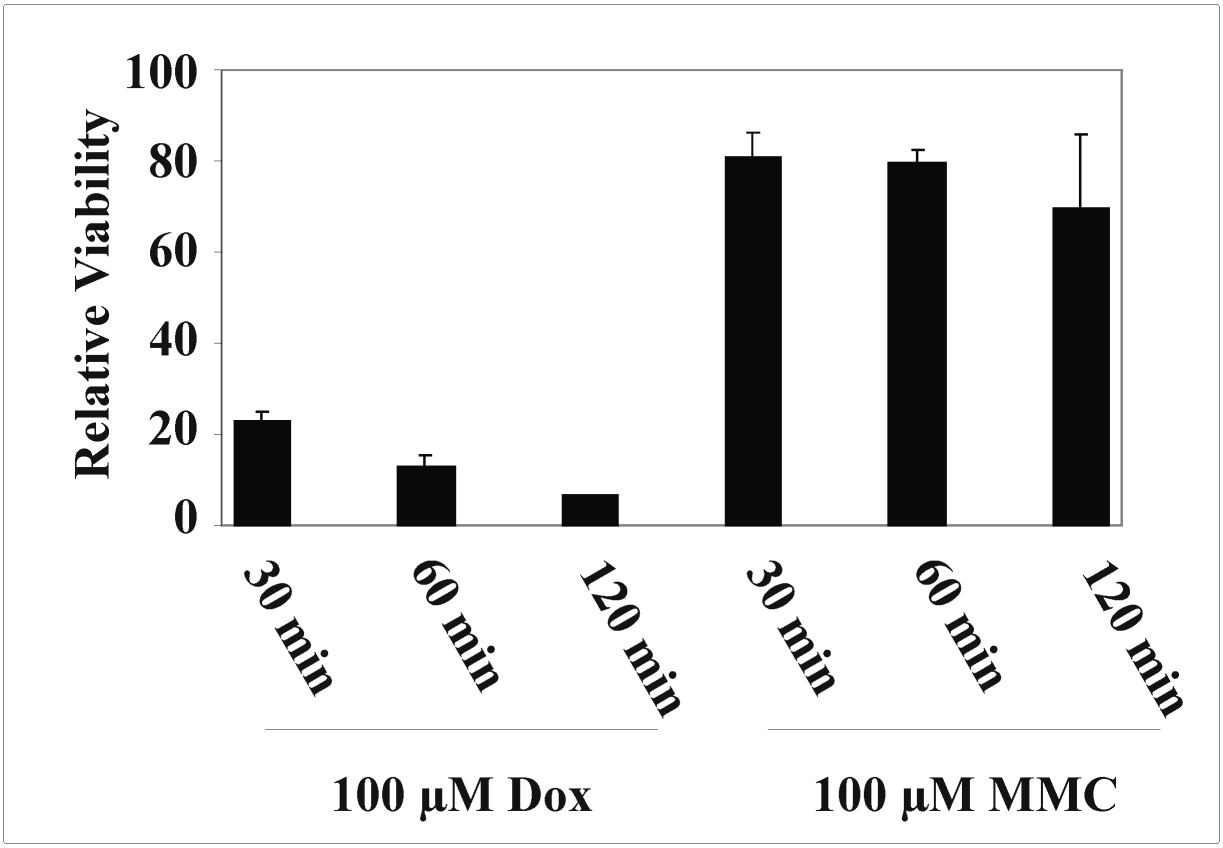

Figure 3.15. Cytotoxicity of doxorubicin and mitomycin C

Cytotoxicity of doxorubicin (Dox) or mitomycin C (MMC) in WB-344 cells. Cells were exposed to 100 µM Dox or MMC for 30, 60 or 120 min, followed by washing and adding DMEM for 24 h.

3.13. Both doxorubicin or MMC induce ERK1/2 activation

Exposure of WB-F344 cells to doxorubicin or MMC for 1h resulted in a strong dual phosphorylation of ERK1/2 in a concentration-dependent manner (Figure 3.16). As demonstrated in Figure 3.15, doxorubicin displayed higher toxicity than MMC. In line with this, higher concentrations of MMC were required to elicit ERK1/2 activation.

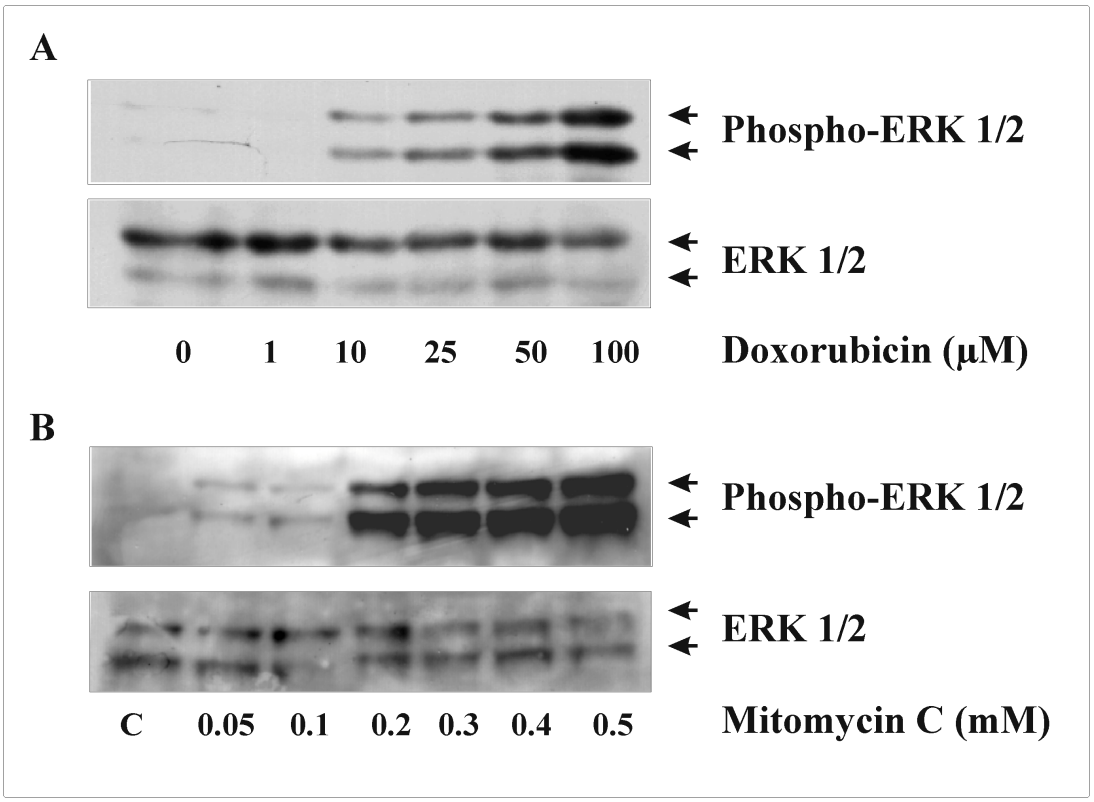

Figure 3.16. Figure 3.2. ERK activation by Doxorubicin and MMC

WB-F344 rat liver epithelial cells were exposed to doxorubicin (A) or MMC (B) in serum free medium at the indicated concentrations for 1h, followed by determination of ERK1/2 phosphorylation and total ERK1/2 levels by Western blotting.

3.14. Role of MEK1/2 and EGFR in doxorubicin or MMC-induced ERK1/2 activation

Cells were incubated with inhibitors or DMSO (control) 30 min prior to exposure to doxorubicin or MMC in the continued presence or absence of the respective inhibitor. U0126, a specific MEK1/2 inhibitor, as well as AG1478 and compound 56, specific EGFR inhibitors, blocked ERK1/2 phosphorylation induced by doxorubicin, revealing the involvement of MEK1/2 and EGFR (Figure 3.17*A*).

U0126 was equally effective in blocking ERK1/2 phosphorylation induced by doxorubicin or MMC within 1h (Figure 3.17*A* and *B*). AG1478 and compound 56 were effective only after 2 h of exposure to MMC (Figure 3.17*C*). In addition to MEK and EGFR inhibitors, AG1295, an inhibitor of the PDGF receptor tyrosine kinase, as well as genistein, a general tyrosine kinase inhibitor and suramin, a general receptor tyrosine kinase inhibitor, were tested in the assay. As expected from the results with EGFR inhibition, pointing to a role of EGFR in MMC-induced ERK1/2, AG1295 did not show any effect on MMC-induced ERK1/2 phosphorylation, excluding a role of the PDGF receptor. Genistein and suramin, however, effectively inhibited ERK1/2 phosphorylation.

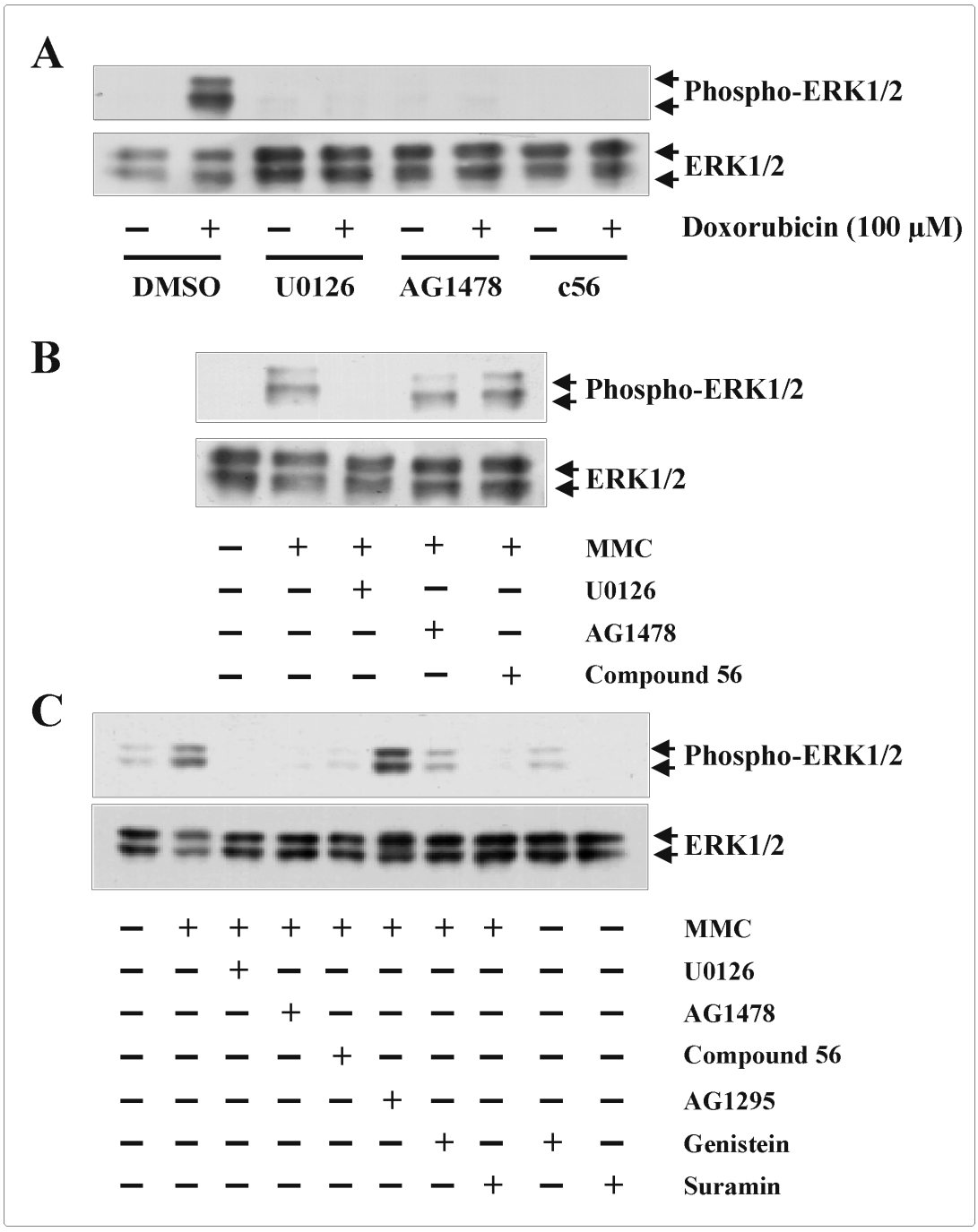

Figure 3.17. The role of EGF receptor and MEK1/2 in doxorubicin- and MMC-induced ERK activation

(A) Cells were pretreated with U0126, AG1478 or compound 56, 10 µM each, for 30 min prior to exposure to 100 µM doxorubicin for 60 min in the absence or continued presence of the respective inhibitors, followed by analysis of ERK1/2 phosphorylation by Western blotting. (B) As in (A), with exposure to MMC. (C) Cells were pretreated with the above inhibitors as well as AG1295 (10 µM), genistein (40 µM), or suramin (500 µM) for 30 min prior exposure to 100 µM MMC for 120 min in the absence or combined presence of the respective inhibitors followed by analysis of ERK1/2 phosphorylation by Western blotting.

3.15. Role of NQOR-1 in doxorubicin and MMC induced ERK activation

To delineate the role of NQOR-1 in ERK1/2 phosphorylation induced by doxorubicin or MMC, dicoumarol was used in the same manner as with the model quinones (see Figure 3.10). Exposure of WB-F344 rat liver epithelial cells to doxorubicin or MMC in the presence of 100μM dicoumarol did not result in ERK1/2 phosphorylation (Figure 3.18), indicating that they undergo two-electron reduction catalysed by NQOR-1. Furthermore, glutathione levels were determined in cells exposed to 100μM doxorubicin for 1h (Figure 3.19*A*). The intracellular level of GSH did not change significantly, excluding alkylation of GSH and pointing to redox cycling as a major mechanism responsible for these doxorubicin effects, which is in line with the tendency to accumulate GSSG (Figures 3.19*B*).

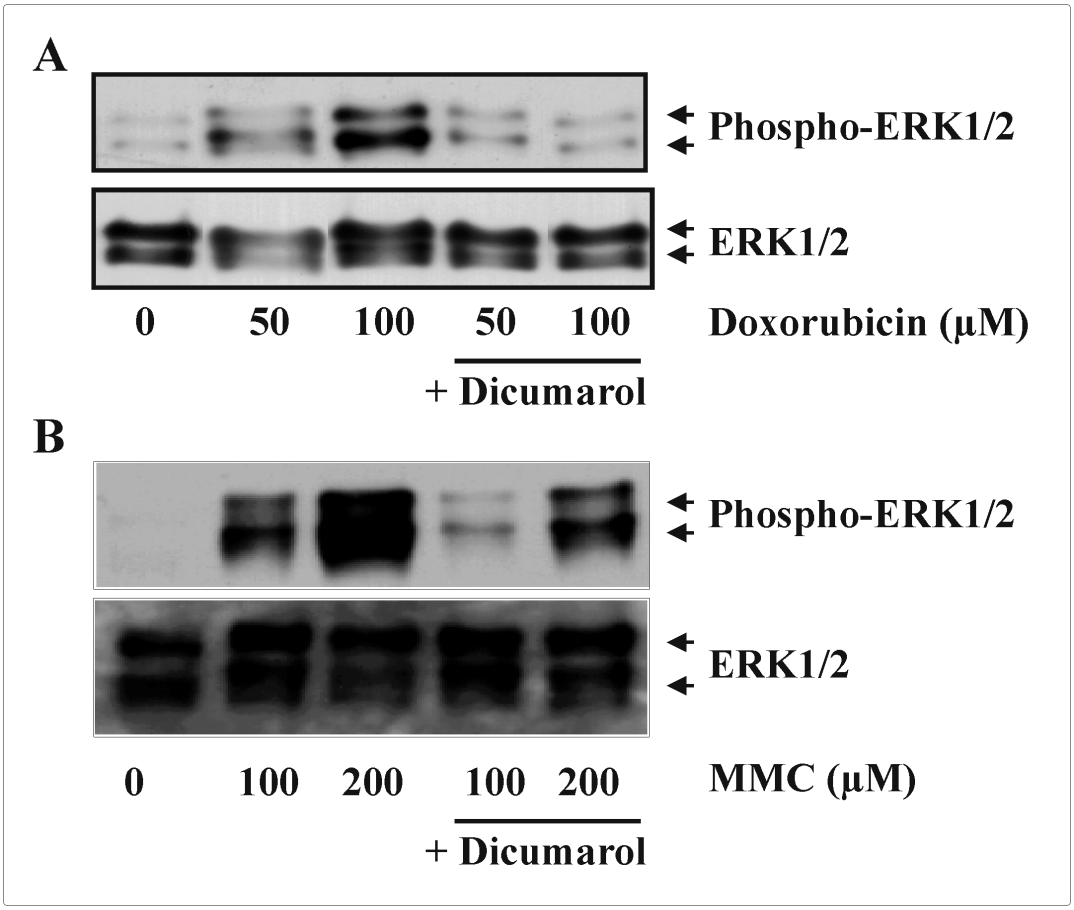

Figure 3. 18. Effect of dicoumarol on ERK1/2 phosphorylation induced by doxorubicin or MMC
Cells were exposed to doxorubicin or MMC at the indicated concentrations for 1h in the presence or absence of dicoumarol (100 μM), followed by analysis of ERK1/2 phosphorylation by Western blotting.

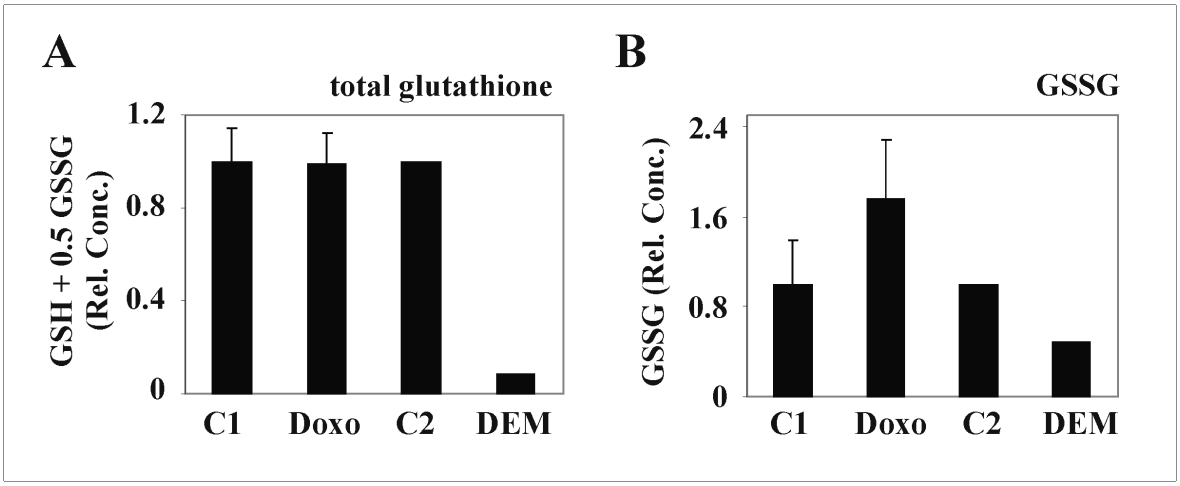

3.19. Relative changes in glutathione levels after exposure of WB-F344 cells to doxorubicin

Cells were exposed to 100 µM doxorubicin or vehicle control, "C1" (H_2O) for 60 min, as well as to 1 mM DEM (positive control) or vehicle control "C2" (DMSO) for 60 min before measuring of total glutathione (A) and GSSG (B) levels. Data are means of 3 and 2 independent experiments performed in triplicate ± S.D in the case of doxorubicin and DEM, respectively.

3.16. Doxorubicin suppresses gap junctional communication (GJC)

Exposure of WB-F344 rat liver epithelial cells to doxorubicin for 1 h resulted in a significant decrease in GJC. This was demonstrated by injecting Lucifer Yellow CH, a fluorescent dye permeating gap-junctional channels, into individual cells in the monolayer. Cells were exposed to the indicated concentrations of doxorubicin, followed by microinjection and counting the number of communicating cells (Figure 3.20*A*). Counting was performed 20 seconds after injection of Lucifer Yellow CH and cell viability controlled using the neutral red assay to confirm that the injected cells were alive and intact (Figure 3.20*B*). The effect of doxorubicin on GJC was also examined by scrape loading with Lucifer Yellow CH. As shown in Figure 3.20*C*, the exposure of WB-F344 cells to doxorubicin led to a pronounced decrease in GJC as the dye transfer was significantly blocked.

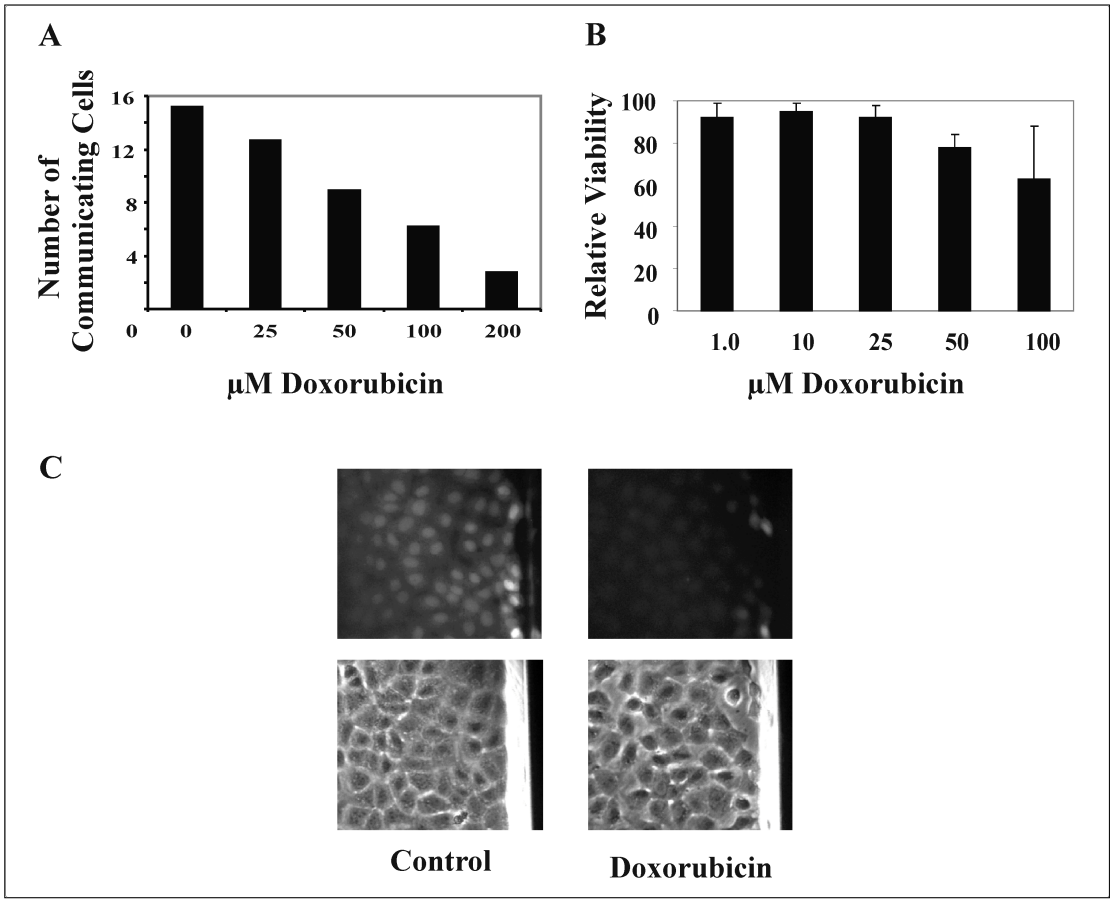

Figure 3.20. Effect of doxorubicin on GJC

(A) GJC analysis by microinjection. WB-F344 rat liver epithelial cells were exposed to doxorubicin for 60 min at the indicated concentrations, followed by extensive washing with PBS and adding serum-free medium directly before analysis of GJC with the Lucifer Yellow CH dye transfer assay. Microinjection was kindly performed by D. Stuhlmann. Data are means of two independent experiments.

(B) Relative cell viability determined with the neutral red (NR) assay. WB-F344 rat liver epithelial cells were exposed to doxorubicin for 60 min at the indicated concentrations followed by washing with PBS and adding the NR solution as described in Materials and Methods. Data are means of three independent experiments.

(C) Scrape loading was performed after cell exposure to 50 µM doxorubicin. The scrapes can bee seen in the right side of each picture. Lucifer Yellow CH could diffuse from cell to cell in the control (top-left) but not in the doxorubicin treated cells (top-right). Phase contrasts pictures demonstrate that WB-F344 cells were intact

3.17. Doxorubicin induces ERK1/2-mediated connexin-43 phosphorylation

GJC may be regulated by phosphorylation of connexin-43, the prominent connexin in WB-F344 cells, which is a known substrate of ERK1/2. Phosphorylation of connexin-43 was analysed by Western blotting and densiometric analysis (Figure 3.21*A*). The subcellular localisation of connexin-43 was monitored by immunohistochemistry (Figure 3.21*B*). Nonphosphorylated and phosphorylated forms were identified from their electrophoretic mobilities. Cells were pretreated with inhibitors or DMSO for 30 min before doxorubicin was added for 1h, followed by Western blot analysis for connexin-43. Doxorubicin induced a shift in electrophoretic mobility (Figure 3-21*A*) and a decrease in the amount of the unphosphorylated protein (P0) band that was almost completely prevented by the inhibitor of MEK1/2, U0126, as well as EGFR inhibitors, AG1478 or compound 56. This indicates that activation of MEK1/2 and ERK1/2 is responsible for the enhanced connexin-43 phosphorylation by doxorubicin. Furthermore, a tendency to depletion of the amount of connexin-43 in the cell membrane was observed by immunohistochemical analysis (Figure 3.20*B*) after exposure to 100 μM doxorubicin for 1 h, pointing to effects other than connexin phosphorylation possibly contributing to the loss of GJC.

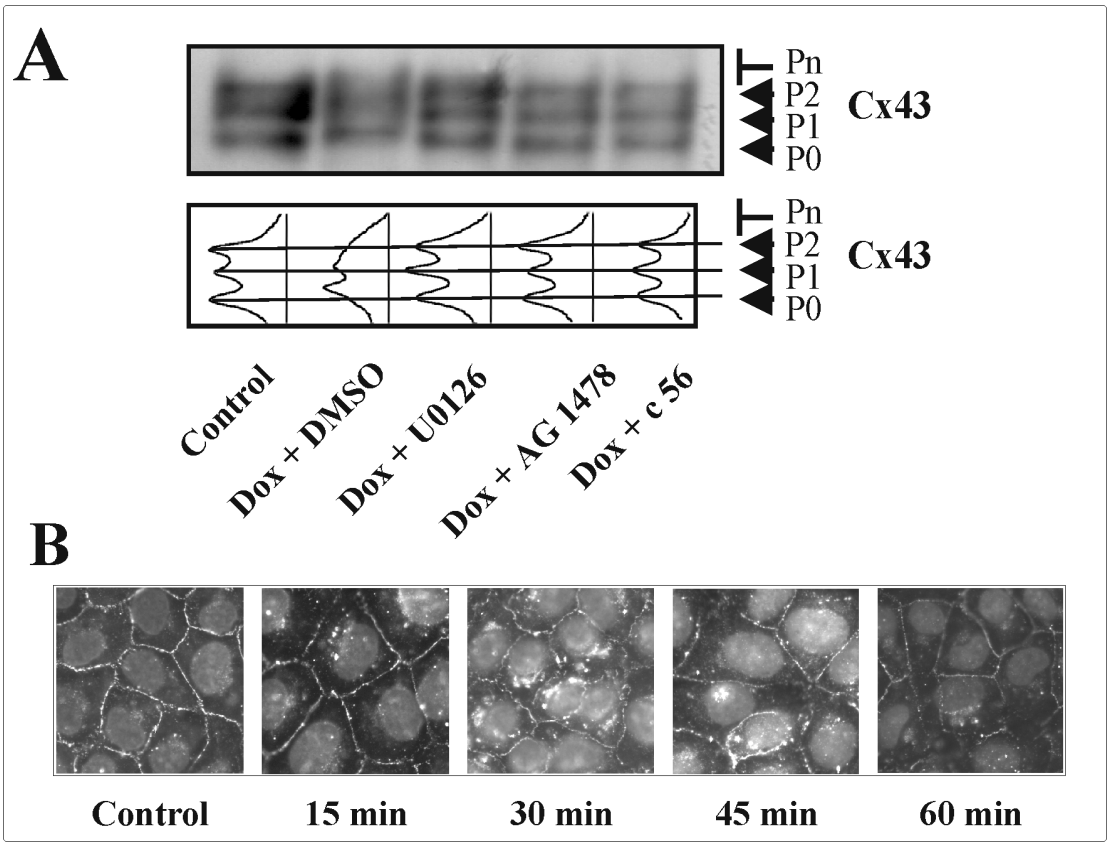

Figure 3.21. Effect of doxorubicin on connexin-43

(A) WB-F344 rat liver epithelial cells were pretreated with U0126, AG1478 or compound 56 (10 µM each) or DMSO (control) for 30 min prior to exposure to 100µM doxorubicin for 1h in the continued presence or absence of the respective inhibitor. Western blot analysis of connexin-43 was performed as described in Materials and Methods. *P0*, unphosphorylated connexin-43; *P1/P2/Pn*, singly, doubly, and hyperphosphorylated connexin-43, respectively. The electrophoretic mobility shift and its reversion are also depicted in densitometric scans (bottom panel).

(B) WB-F344 rat liver epithelial cells were exposed to doxorubicin (100 µM) for the times indicated, (control 1 h without doxorubicin) followed by immunohistochemical analysis to monitor the subcellular localisation of connexin-43. Nuclei were stained with DAPI for orientation.

3.18. Inhibition of ERK1/2 activation prevents the loss of GJC induced by doxorubicin

EGFR and MEK/ERK were shown to be involved in connexin-43 hyperphosphorylation upon exposure to doxorubicin as demonstrated by Western blot analysis (Figure 3.17). If loss of GJC is due mainly to connexin phosphorylation, then inhibition of either of these kinases should prevent the decrease in GJC induced by

doxorubicin. It was recently reported that menadione leads to decreased GJC that is regained in the presence of EGFR or MEK1/2 inhibitors (Klotz 2002b). Likewise, cell exposure to 50 µM doxorubicin for 60 min resulted in a decrease in GJC of about 50% of vehicle (DMSO/H_2O)-treated control cells. In the presence of U0126, AG1478 or compound 56, 10 µM each, the GJC was largely regained (Figure 3.22*A*). Figure 3.22*B* shows pictures taken from cells after microinjection of Lucifer Yellow CH. Cells exposed to doxorubicin displayed a very low level of communication: the fluorescent dye could not diffuse to neighboring cells. In the presence of U0126, the communication level was re-established. The same results as with U0126 were obtained in the presence of AG1478 or c 56 (not shown). Scrape loading with Lucifer Yellow CH yielded similar results, with doxorubicin preventing dye spreading beyond the layer of scraped cells and MEK/EGFR inhibitors restoring communication (Figure 3.22*C*).

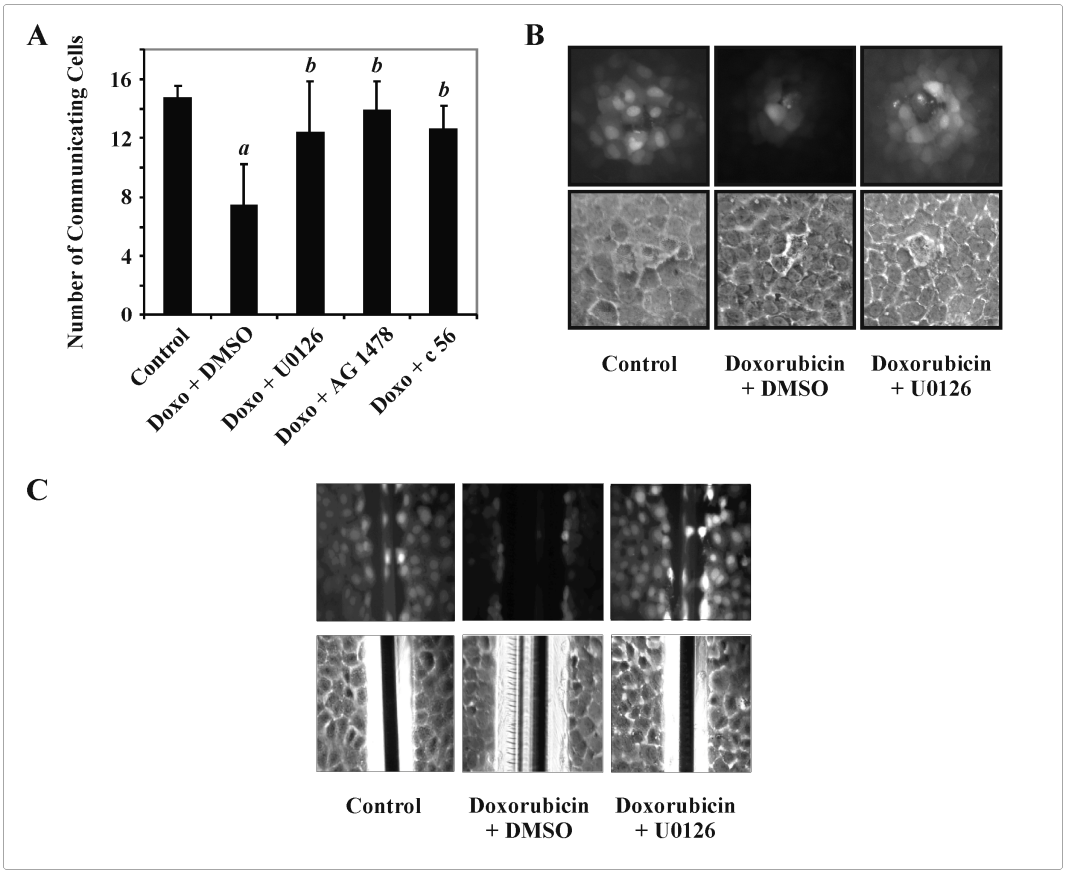

Figure 3. 22. GJC after exposure to doxorubicin

Cells were exposed to 50 µM doxorubicin in the absence or presence of U0126, AG1478 or compound 56 (10 µM each) for 60 min, followed by analysis of GJC by dye transfer analysis. Cells were pretreated with inhibitors or vehicle (DMSO) for 30 min prior the addition of doxorubicin. a, significantly different from control; b, significantly different from a (Doxo + DMSO). The number of communicating cells was counted 20 seconds after injection of Lucifer Yellow CH. (B) Fluorescent images (top) and their corresponding phase contrast images (bottom) after microinjection of Lucifer Yellow CH into WB-F344 cells after treatment with doxorubicin (50 µM) in presence or absence of U0126. Images were taken 20 seconds after injection. (C) Fluorescent images (top) and the corresponding phase contrast pictures (bottom) of WB-F344 cells scrape-loaded with Lucifer Yellow CH after treatment with doxorubicin (50 µM) in the presence or absence of U0126. Images were taken after incubation for 2 min with Lucifer Yellow CH. Microinjection was kindly performed by D. Stuhlmann.

3.19. The role of ERK5 in doxorubicin-induced connexin-43 phosphorylation

ERK5 is another mitogen-activated protein kinase that has recently been proposed to be the major mediator of EGF-induced connexin-43 phosphorylation and downregulation of GJC (Scott et al, 2003). Therefore, the role of ERK5 in doxorubicin-induced connexin-43 phosphorylation in WB-F344 cells was tested.

Cells were exposed to doxorubicin for 15 or 60 min, followed by Western blot analysis of ERK5 phosphorylation. EGF, a known stimulator of ERK5 phosphorylation (Mody et al, 2001) was taken as a positive control. Interestingly, EGF (100 ng/ml) was found to strongly phosphorylate ERK5 and ERK1/2, while doxorubicin only induced the phosphorylation of ERK1/2 but not ERK5 (Figure 3.23*A*).

PD184352 is a potent inhibitor of MEK1/2 and MEK5 that is able to inhibit the phosphorylation of ERK1/2 at 2 μM and both ERK5 and ERK1/2 at 10 μM in HeLa cells (Mody et al, 2001). WB-F344 cells were pretreated with PD184352 (2 or 10 μM) for 30 min before exposure to doxorubicin (100 μM) for 60 min followed by Western blot analysis of phospho-ERK1/2. PD98059, a known inhibitor of MEK1/2, was used as a positive control. PD184352 effectively blocked ERK1/2 activation induced either by EGF or doxorubicin (Figure 3.23*B*), but it was not able to inhibit ERK5 phosphorylation induced by EGF (Figure 3.23*C*). Together with the finding that doxorubicin did not phosphorylate ERK5, these data point to ERK5 not being of any importance for doxorubicin-induced connexin-43 phosphorylation. In line with this, PD184352 (2 μM) effectively inhibited the loss of GJC induced by doxorubicin (50 μM) (Figure 3.23*D*). These data indicate that ERK1/2 is in charge of modulating GJC in WB-F344 cells exposed to doxorubicin and is more important than ERK5.

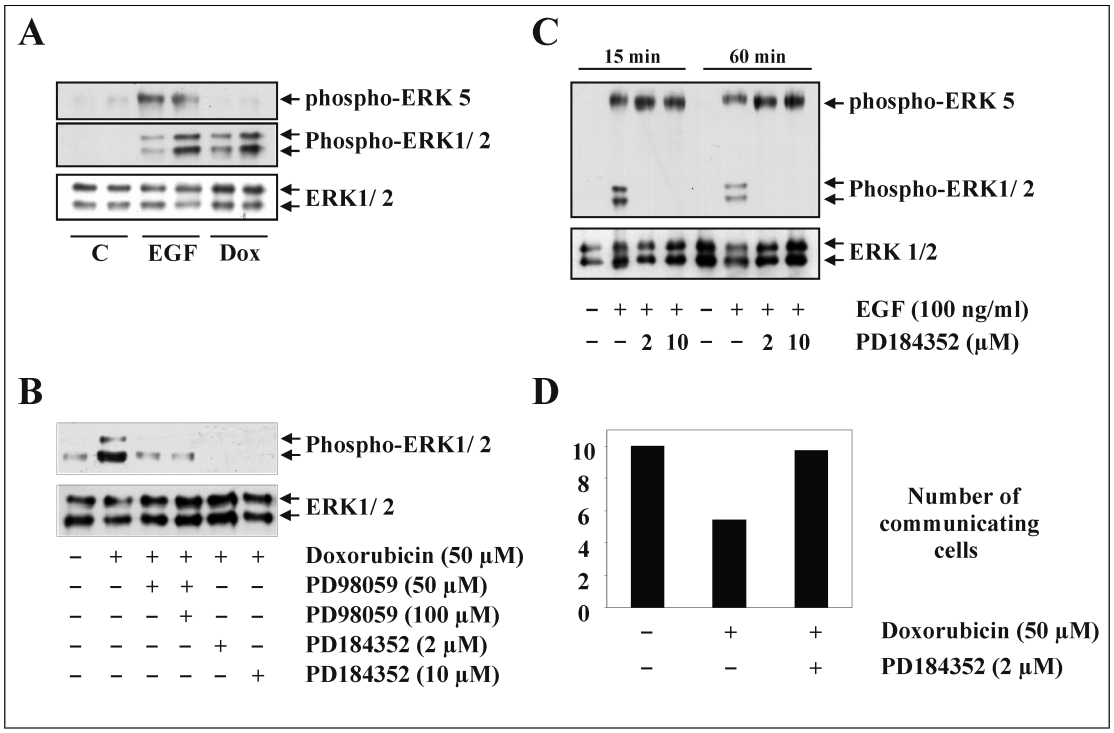

Figure 3.23. Doxorubicin-induced loss in GJC is not mediated by ERK5

(A) EGF but not doxorubicin activates ERK5. Cells were exposed to EGF (100 ng/ml) or doxorubicin (50 µM) for 1h, followed by Western blot analysis of ERK5 and ERK1/2 phosphorylation. A pan-ERK antibody was used to control for the presence of total ERK.

(B) PD184352 effectively inhibits ERK1/2 phosphorylation. PD98059 was taken a positive control for MEK/2 inhibition. Cells were pretreated with PD184352, PD98059 or DMSO for 30 min, followed by cell exposure to doxorubicin in the presence or absence of the inhibitors for 1h.

(C) PD184352 effectively inhibits ERK1/2 but not ERK5 phosphorylation induced by EGF. Cells were pretreated with PD184352 (2 or 10 µM) for 30 min prior to exposure to EGF (100 ng/ml) for 15 min or 1h, followed by Western blot analysis of ERK5 and ERK1/2 phosphorylation.

(D) PD184352 prevents the loss of GJC induced by doxorubicin. Cells were pretreated with 2 µM PD184352 prior to exposure to doxorubicin (50 µM) for 1h, followed by microinjection using Lucifer Yellow CH as described in Materials and Methods. In summary, ERK1/2 is the key player in the downregulation of GJC induced by doxorubicin. Microinjection was kindly performed by D. Stuhlmann.

3.20. Prevention of the doxorubicin-induced loss of GJC may enhance its toxicity

WB-F344 cells have shown little ability to communicate through gap junctions after treatment with doxorubicin. U0126 restored the loss in GJC and reversed the doxorubicin-induced connexin-43 phosphorylation (Figure 3.21 and 3.22). What would be the effect of MEK/EKK1/2 inhibition on the toxicity of doxorubicin?

Cells were exposed to the indicated concentrations of doxorubicin in the absence or continued presence of U0126 for 24 h, followed by neutral red assay to determine the toxicity of doxorubicin. Interestingly, the toxicity of doxorubicin increased in the presence of U0126 (Figure 3.24). This could be due to the restoration of GJC by U0126, thus allowing the drug to diffuse from cell to cell, enhancing its toxicity.

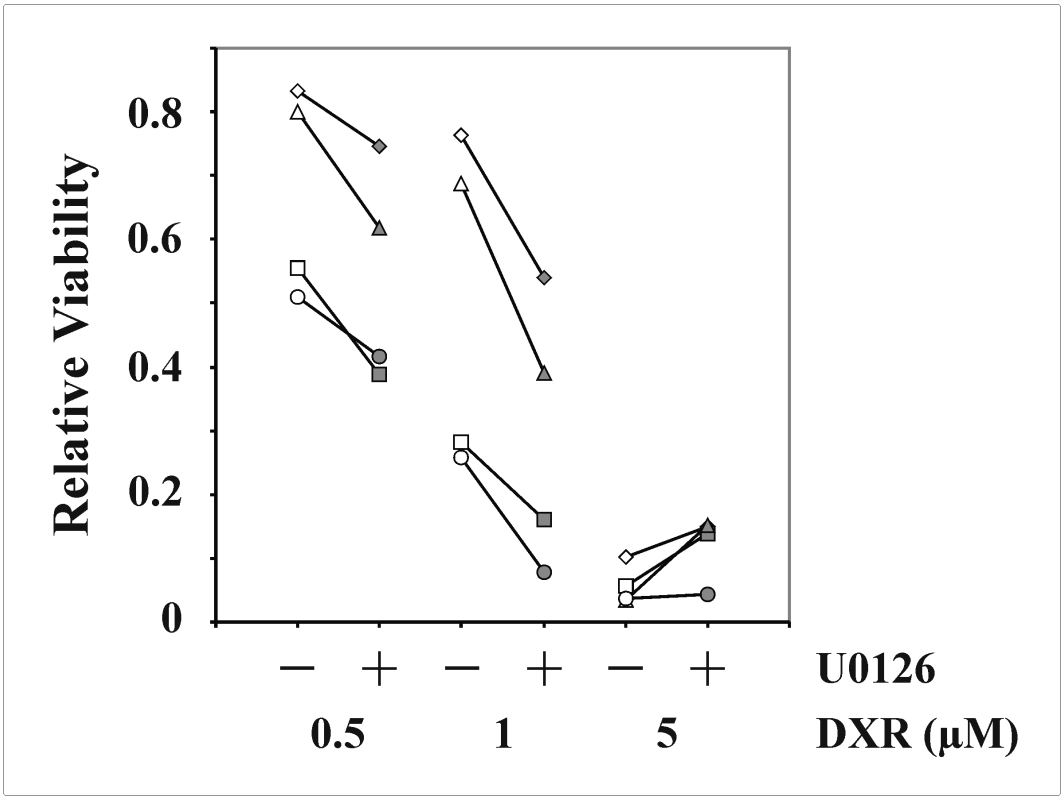

Figure 3.24. Doxorubicin cytotoxicity in the presence or absence of U0126

WB-344 cells were pretreated with or without U0126 for 30 min and then exposed to 0.5, 1.0 or 5.0 μM doxorubicin for 24 h in the absence (open figures) or presence (closed figures) of U0126. Doxorubicin (0.5 and 1.0 μM) displayed higher toxicity in presence of U0126. Data are comprised from 4 independent experiments.

4. Discussion

4.1. Significance of ERK activation by quinones

Activation of ERK1/2 is usually connected with cell proliferation, which is due to the substrates of the kinases, including transcription factors as well as key enzymes involved in nucleotide and protein synthesis (see Whitmarsh and Davis, 2000, for review). As shown in Figures 3.4 and 3.16, both model quinones (MQ, BQ and DMNQ) and chemotherapeutic quinones (doxorubicin and MMC) activate ERK1/2.

4.2. Connexin-43 is phosphorylated by ERK1/2 but not ERK5

ERK1/2 phosphorylation results in an attenuation of GJC (Warn-Cramer et al., 1996, Lampe and Lau, 2000 and Kim et al., 1999). Three connexin-43 sites were demonstrated to be phosphorylated by ERK1/2, Ser255 as well as Ser279/Ser282, all of which are located in the C-terminal cytoplasmic domain of the protein (Figure 4.1) (Warn-Cramer et al., 1996 and Lampe and Lau 2000). Menadione as well as BQ and DMNQ all activate ERK1/2, resulting in the phosphorylation of connexin-43 at Ser 279/282 (Figures 3.9 and 4.1).

As with model quinones, the chemotherapeutic quinone doxorubicin also activates ERK1/2 (Figure 3.16), resulting in a decrease in GJC (Figures 3.20 and 3.22) that was demonstrated to be due to phosphorylation of connexin-43 (Figures 3.21*A*). This phosphorylation was prevented by U0126, AG1478 or compound 56 (Figure 3.21*A*), and the same three inhibitors also prevented the decline in GJC (Figure 3.22*A*), indicating that the pathway that leads to connexin-43 phosphorylation is from EGFR *via* MEK and ERK (summarised in Figure 4.2).

Other MAPK, such as the stress-activated JNK (c-Jun N-terminal kinase) and p38, were demonstrated to also directly inhibit GJC (Polontchouk et al., 2002 and Petrich et al., 2002), indicating that the MAPK family members are generally in charge of controlling GJC. Another member of the MAPK family is ERK5, also known as big mitogen- activated protein kinase-1 (BMK1), that was recently demonstrated to phosphorylate connexin-43 at S255 (Scott et al., 2003).

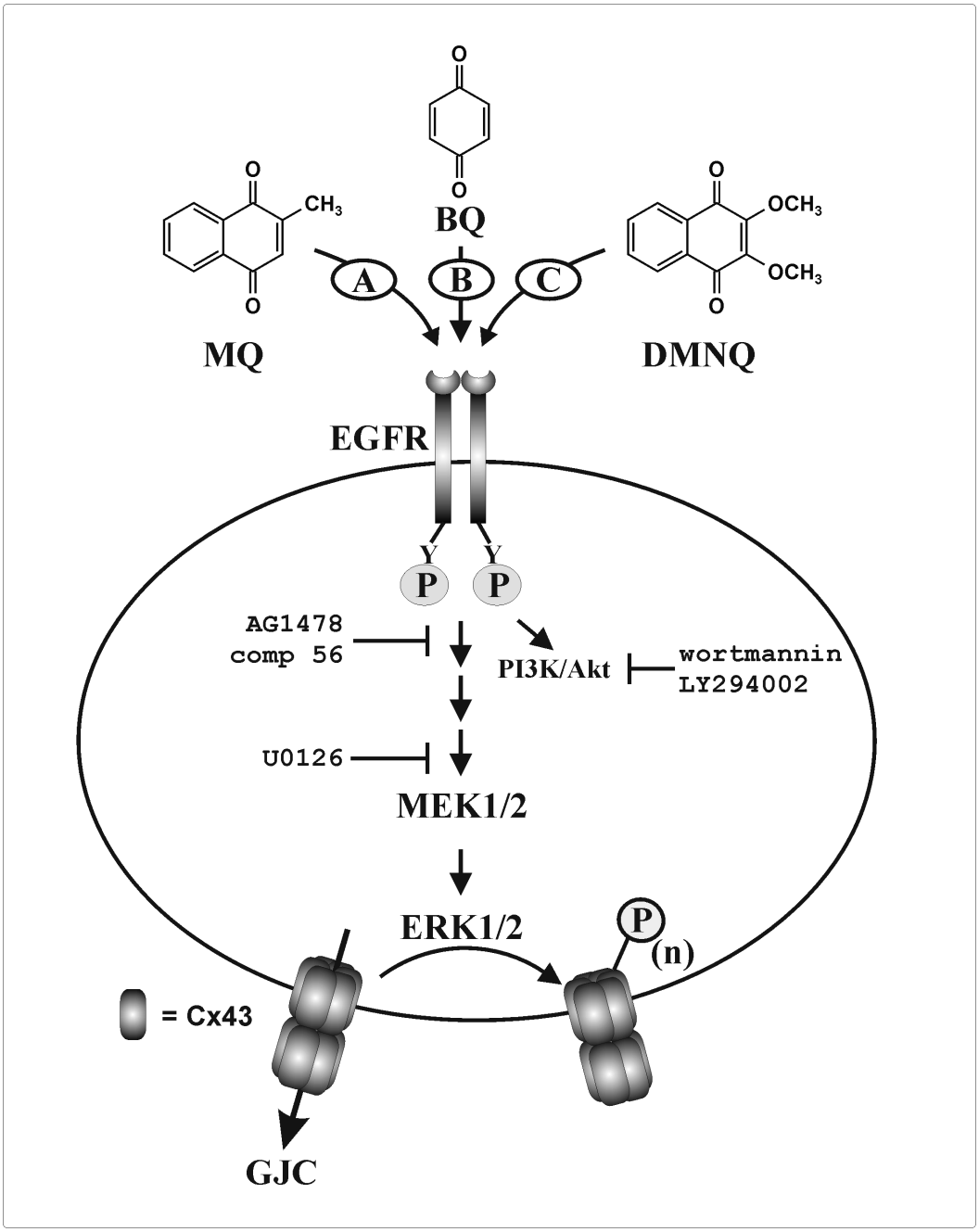

Figure 4.1. Cellular responses to quinones

Funnelling of cellular responses to quinones into epidermal growth factor receptor (EGFR)-dependent signaling, resulting in phosphorylation of connexin-43 and loss of gap junctional communication (GJC). The three different quinones, the alkylating and redox cycling menadione (*A*), the strong alkylator BQ (*B*) and the exclusive redox cycler DMNQ (*C*), activate distinct signaling mechanisms converging at the level of EGFR activation and leading to the phosphorylation of connexin-43.

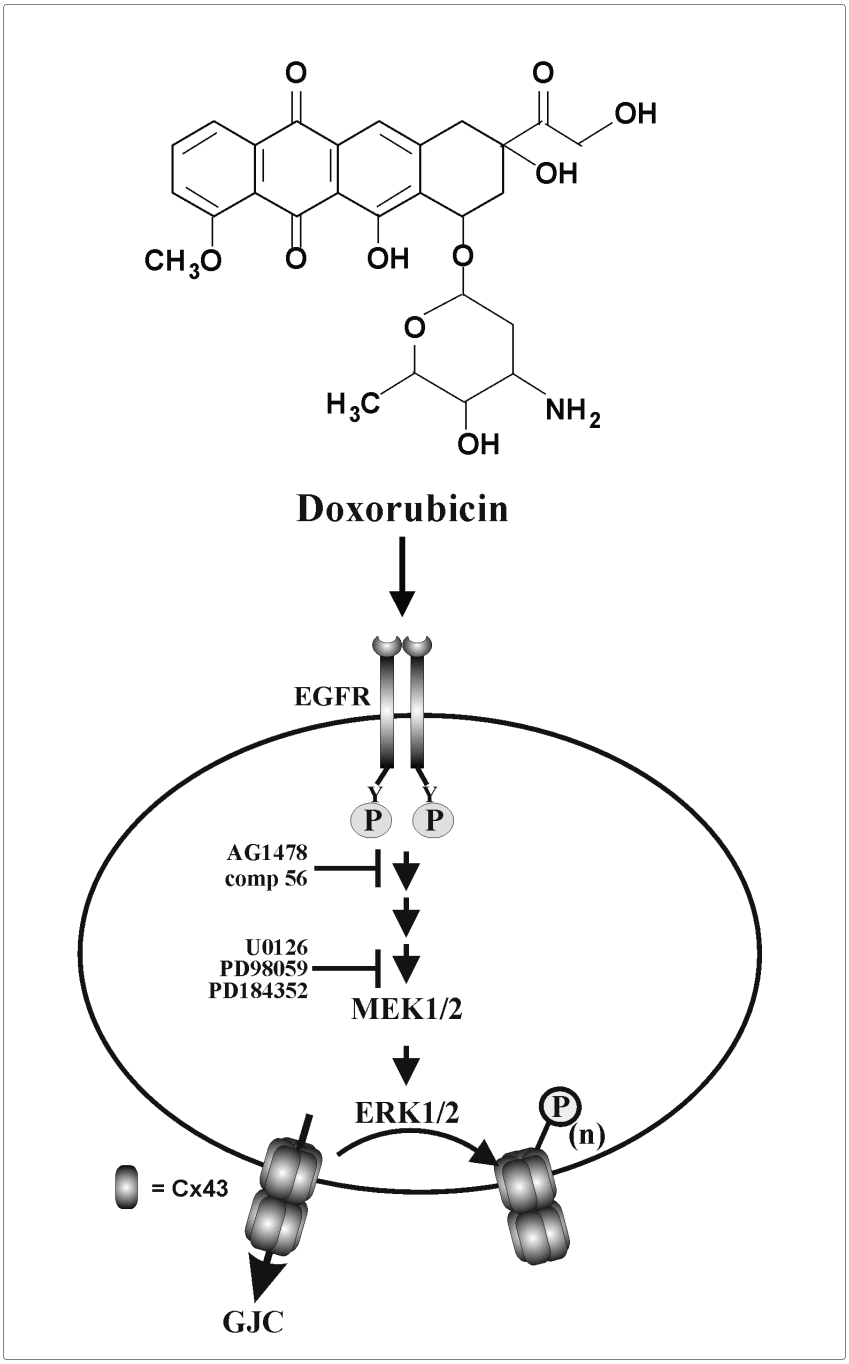

Figure 4.2. Cellular responses to doxorubicin

Cellular responses to quinones in epidermal growth factor receptor (EGFR)-dependent signaling, resulting in phosphorylation of connexin-43 and loss of gap junctional communication (GJC).

In the case of doxorubicin ERK5 was not stimulated although it was potently induced by EGF (Figure 3.23*A*), indicating that ERK5 is not involved in the loss of GJC induced by doxorubicin. Furthermore, PD184352, a known potent inhibitor of ERK1/2 but not ERK5 activation at 2 μM (Mody et al., 2001), strongly attenuated ERK1/2 phosphorylation induced both by doxorubicin or EGF (Figure 3.22*B* and *C*). In addition, 2 μM PD184352 were able to prevent the loss in GJC induced by doxorubicin (Figure 3.23*D*).

Exposure of cancerous tissue to a drug like doxorubicin is aimed at killing the respective cells. If, however, the very agent employed induces connexin phosphorylation, thus impairing GJC, the outcome of chemotherapy might be sub-optimal because the diffusion between cytoplasms would be impaired. This is of significance for cancer chemotherapy approaches exploiting the so-called bystander effect that is based upon the direct diffusion of active drug between the cytoplasms of metabolically active adjacent cells. As this diffusion is prevented by the cellular reaction to the quinone itself, i.e. by the induced connexin-43 phosphorylation and decreased GJC, a possible approach to enhance efficiency of quinone-based chemotherapy may be to pharmacologically block the EGFR-ERK-connexin-43 pathway in cells exposed to the quinoid agent.

A preliminary investigation in this direction was performed and indeed, as shown in Figure 3.24, the toxicity of doxorubicin increased in the presence of U0126, a specific inhibitor of MEK1/2 activation that has been shown to impair ERK1/2 (Figure 3.17*A*) and connexin-43 phosphorylation (Figure 3.21*A*) as well as to prevent the decline in GJC induced by doxorubicin (Figure 3.22).

4.3. Quinones are possessing different mechanisms converging at the level of EGFR activation

Receptor tyrosine kinases such as the EGFR or the PDGF receptor forms appear to be activated by a variety of stressful stimuli, mediating activation of downstream signaling events in the absence of the respective ligands. Such stimuli include several different reactive oxygen and nitrogen species, such as hydrogen peroxide (Wang et al., 2000) or peroxynitrite (Klotz et al., 2000), as well as heavy metal ions (Wu et al., 1999) or anti-cancer agents such as cisplatin (Benhar et al., 2002).

4.3.1. Proposed mechanism for the activation of EGFR-dependent signaling by menadione

How should menadione and other quinones lead to activation of the EGFR and of downstream signaling? A hypothesis that is widely accepted for the activation of EGFR signaling by reactive oxygen species is the inactivation of a phosphotyrosine phosphatase (or protein tyrosine phosphatase; PTPase) negatively regulating the EGFR (Herrlich and Böhmer, 2000). Indeed, isolated PTPases have been shown to be inhibited by menadione (Klotz et al., 2002b) as well as other naphthoquinone derivatives (Carr et al., 2002). Recently, it was demonstrated that menadione also blocks PTPase activity in a cellular environment (Abdelmohsen et al., 2003).

In the case of menadione, direct alkylation of a PTPase can be proposed as a possible major mechanism for PTPase inactivation and EGFR stimulation. First, menadione-induced ERK activation was demonstrated to be independent of NAD(P)H:quinone oxidoreductase-1 (Figure 3.10) as dicoumarol did not impair menadione-induced ERK1/2 activation, thus excluding redox cycling as a major mechanism. Secondly, menadione may directly interact with isolated as well as cellular PTPases (Klotz et al., 2002b and Abdelmohsen et al., 2003); thirdly, incubation of cells with NAC prior to exposure to menadione did not impair ERK activation by the quinone (different from BQ and DMNQ; Figure 3.12*B*), excluding GSH depletion as a major factor.

Although redox cycling of menadione does not appear to be involved in ERK activation, it does occur, as an extensive accumulation of GSSG was observed in menadione-treated cells. That might be explained by redox cycling of menadione in combination with its known inhibitory effect on glutathione reductase (Bellomo, 1987). Superoxide derived from redox cycling would yield hydrogen peroxide that is reduced by glutathione peroxidase at the expense of GSH which, in turn, ends up as GSSG that cannot be reduced by glutathione reductase if menadione is present (Figure 4.3).

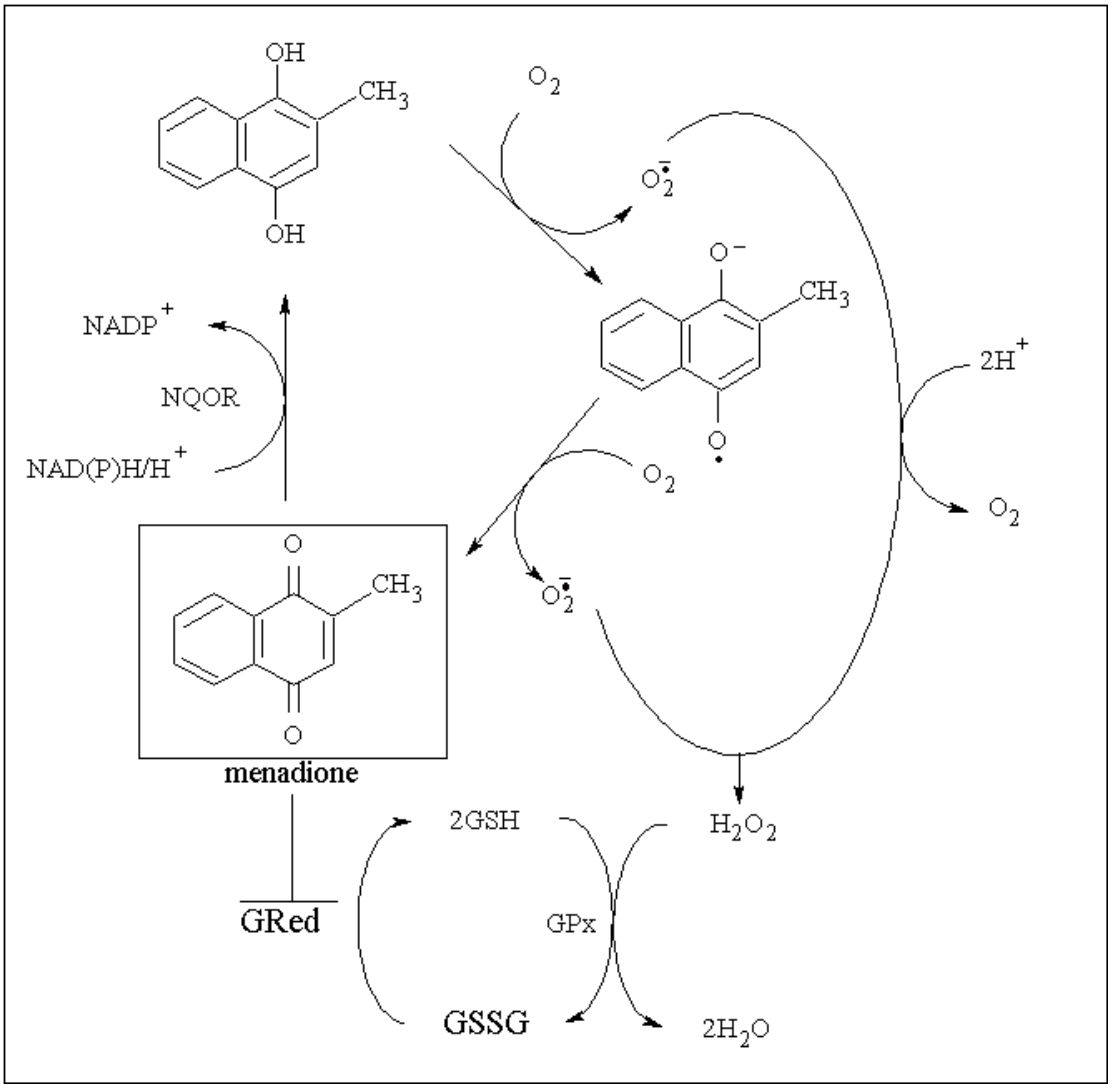

Figure 4.3. A proposed mechanism for GSSG accumulation induced by menadione

Redox cycling of menadione ultimately leads to the formation of hydrogen peroxide (H_2O_2) that is reduced by glutathione peroxidase (GPx) at the expense of 2GSH which, in turn, end up as GSSG. The latter cannot be reduced by glutathione reductase (GRed) due to its inhibition by menadione.

4.3.2. Proposed mechanism for the activation of EGFR-dependent signaling by *p*-benzoquinone

An indirect mechanism might also be considered that depends on GSH. A depletion of cellular GSH such as by BQ or DEM might render PTPases and other oxidant-sensitive signaling proteins prone to oxidative inactivation.

Thioredoxins or peroxiredoxins are examples for proteins known for their regulatory role in redox signaling. Like PTPases, they harbor thiolates at their reactive sites and can be oxidized to sulfenic acids by metabolically generated H_2O_2 (Dickinson and

Forman, 2002). The sulfenic acids can be reduced by GSH, leading to reactivation of the proteins. If, however, cellular GSH levels are strongly diminished, such as with BQ and DEM (Figure 3.11*B*), reduction and reactivation are impaired.

4.3.3. Proposed mechanism for the activation of EGFR-dependent signaling by DMNQ, doxorubicin and MMC

DMNQ, undergoing redox cycling, does neither inactivate a PTPase (Abdelmohsen et al., 2003) nor significantly deplete GSH levels in the cell within 15 min (Figure 3.11*B* top), the time required to see activation of the signaling pathways investigated. In addition, ERK1/2 activation was impaired in the presence of dicoumarol (Figure 3.10*B*), pointing to the important role of NQOR-1. Therefore, it may be speculated that redox cycling of DMNQ may be the source of superoxide and hydrogen peroxide that consequently oxidize signaling proteins such as the aforementioned, entailing effects identical to those seen under conditions with depleted GSH levels.

The same can be speculated in the cases of doxorubicin and MMC; the activation of ERK1/2 by both is blocked by dicoumarol (Figure 3.18), again pointing to the important role of NQOR-1 in the metabolism of these chemotherapeutic drugs. Furthermore, doxorubicin was not able to deplete intracellular glutathione (Figure 3.19), indicating that it is unable to effectively alkylate the cellular thiols such as glutathione or protein thiols, reflecting its inability to inhibit PTPases. Thus, redox cycling could be the major cellular mechanism of action of doxorubicin.

5. Summary

The effect of redox cycling and alkylating quinones on epidermal growth factor receptor (EGFR) dependent signaling pathways and consequences thereof were investigated. Rat liver epithelial cells were exposed to three quinones with different properties: menadione (2-methyl-1,4-naphthoquinone, vitamin K_3), an alkylating as well as redox-cycling quinone, the strongly alkylating *p*-benzoquinone (BQ) and the non-arylating redox-cycler, 2,3-dimethoxy-1,4-naphthoquinone (DMNQ).

All three quinones induced the activation of extracellular signal-regulated kinase (ERK) 1 and ERK 2 *via* activation of epidermal growth factor receptor (EGFR) and MAPK/ERK kinases (MEK) 1/2. ERK activation resulted in phosphorylation at Ser279 and Ser282 of the gap junctional protein, connexin-43, known to result in loss of gap junctional intercellular communication (GJC). Another EGFR-dependent pathway was stimulated by the quinones, leading to activation of the antiapoptotic kinase Akt *via* phosphoinositide 3-kinase. Intrestingly, activation of EGFR-dependent signaling by these quinones occurred through different mechanisms: (i) menadione, but not BQ or DMNQ, inhibited a protein tyrosine phosphatase (PTPase) regulating the EGFR, as concluded from an EGFR-dephosphorylation assay; (ii) while menadione-induced activation of ERK was unimpaired by pretreatment of cells with N-acetyl cysteine, activation by BQ and DMNQ was prevented; (iii) cellular glutathione (GSH) levels were strongly depleted by BQ. The mere depletion of GSH by application of diethyl maleate EGFR-dependently activated ERK and Akt, thus mimicking BQ effects. GSH levels were only moderately decreased by menadione and not affected by DMNQ.

The chemotherapeutic quinones doxorubicin and mitomycin C also activated ERK1/2 *via* activation of EGFR and MEK1/2. Activation of this cascade by these quinones as well as by DMNQ was demonstrated to be dependent on NAD(P)H:quinone oxidoreductase-1, pointing to an important role of redox cycling in the process leading to activation of the signaling cascade. Cell exposure to doxorubicin led to a dose-dependent decrease in GJC that was due to phosphorylation of connexin-43 by ERK1/2. By contrast, ERK5 was not involved. In summary, different quinones affect the same signaling pathway leading to the regulation of intercellular communication, converging at the level of EGFR.

6. References

Abdelmohsen, K., Gerber, P.A., von Montfort C., Sies, H., and Klotz. L-O. (2003). Epidermal growth factor receptor is a common mediator of quinone-induced signaling leading to phosphorylation of connexin 43: role of glutathione and tyrosine phosphatases. *J. Biol. Chem.* **40**, 38360-38367

Agus, D.B., Bunn, P.A., Franklin, W., et al. (2000). HER-2/neu as a therapeutic target in non-small cell lung cancer. *Semin. Oncol.* **27**, 53-63, (Suppl 11)

Ahn, N.G., Seger, R., and Krebs, E.G. (1992). The mitogen-activated protein kinase activator. *Curr. Opin. Cell Biol.* **4**, 992-999

Akerboom, T., Bikzer, M., and Sies, H. (1982). The relationship of billary glutathione disulfide efflux and intracellular glutathione disulfide content in perfused rat liver. *J. Biol.Chem.* **257**, 4248-4252

Alroy, I., and Yarden, Y. (1997). The ErbB signaling network in embryogenesis and oncogenesis: Signal diversification through combinatorial ligand-receptor interactions. *FEBS LETT*. **410** (1), 83-86

Anderson, M.E. (1985). Determination of glutathione and glutathione disulfide in biological samples. *Methods in enzymology.* **113**, 548-555

Ann, M. (1986). Induction of DT Diaphorase and functionally related enzymes by anti-carcinogenic and anti-toxic compounds. *Chemica scripta.* **27A**, 67-69

Arif, J.M., Lehmler, H.J., Robertson, L.W., and Gupta, R.C. (2003). Interaction of benzoquinone- and hydroquinonederivatives of lower chlorinated biphenyls with DNA and nucleotides in vitro. *Chemico-biological interactions.* **142** (3), 307-316

Aronheim, A., Engelberg, D., Li, N., al-Alawi, N., Schlessinger, J., and Karin, M. (1994). Membrane targeting of the nucleotide exchange factor Sos is sufficient for activating the Ras signaling pathway. *Cell.* **23**, 949-961

Miral, D. (1998). *DNA & free radicals, techniques, mechanisms and applications*, Chapter one, Mechanisms of free radical damage to DNA, pages 3-26

Baselga, J. (2002). Targeting the epidermal growth factor receptor with tirosine kinase inhibitors: small molecules, big hopes. *J. Clin. Oncol.* **20**, 2217-2219

Bellacosa, A., Testa, J.R., Staal, S.P., and Tsichlis, P.N. (1991). A retroviral oncogene, akt, encoding a serine-threonine kinase containing an SH2-like region. *Science.* **11**;254(5029):274-7

Bellomo, G., Mirabelli, F., DiMonte, D., Richelmi, P., Thor, H., Orrenius, C., and Orrenius, S. (1987). Formation and reduction of glutathione-protein mixed disulfides during oxidative stress. A study with isolated hepatocytes and menadione (2-methyl-1,4-naphthoquinone). *Biochem. Pharmacol.* **36**, 1313-1320

Benhar, M., Engelberg, D., and Levitzki, A. (2002). Cisplatin-induced activation of the EGF receptor. *Oncogene.* **12**, 8723-8731

Boatman, R.J., English, J.C., Perry, L.G., and Fiorica, L.A. (2000). Covalent protein adducts of hydroquinone in tissues from rats: Identification and quantitation of sulfhydryl-bound forms *Chem. Res. Toxicol*. **13**,853-860

Bolton, J.L., Trush, M.A., Penning, T.M., Dryhurst, G., and Monks, T.J. (2000). Role of quinones in toxicology. *Chem. Res. Toxicol.* **13**, 135-160

Bruce, A., and Powis, G. (1981). Pulse radiolysis studies of antitumor quinones: Radical lifetimes, reactivity with oxygen, and one-electron reduction potentials. *Arch. Biochem. Biophys.* **209**, 119-126

Brunmark, A., and Cadenas, E. (1989). Redox and addition chemistry of quinoid compounds and its biological implications. *Free Radic. Biol. Med*. **7**, 435-477

Cadena, D.L., and Gill, G.N. (1992). Receptor tyrosine kinases. *FASEB J.* **6**, 2332-2337

Calabresis, P., and Chabner, B. (1996). *The pharmcological basis of therapeutics*, **9th Ed**. Section X, Chemotherapy of Neuroplastic Diseases, pages 1225-1232

Carr, B.I., Wang, Z., and Kar, S. (2002). K vitamins, PTP antagonism, and cell growth arrest. *J. Cell Physiol.* **193**, 263-274

Chabner, A., Carmen, J., Allegra, A., and Calabresi. (1996). *The pharmcological basis of therapeutics*. **9th Ed**. Chapter 51, pages 1233-1286

Christopher, P., Wei L., Diane, M., Stephen, S., Michael, S., and Kuida, K. (2002). Erk5 null mice display multiple extraembryonic vascular and embryonic cardiovascular defects. *Proc. Nat. Acad. Sci.* **99**, 9248-9253

Ciardiello, F., and Tortora, G. (2001). A novel approach in the treatment of cancer: targeting the epidermal growth factor receptor. *Clin Cancer Res*. **7**, 2958-2970

Dent, P., Haser, W., Haystead, T.A., Vincent, L.A., Roberts, T.M., and Sturgill, T.W. (1992). Activation of mitogen-activated protein kinase kinase by v-Raf in NIH 3T3 cells and in vitro. *Science.* **257**, 1404-1407

Dickinson, D.A., Forman, H.J. (2002). Glutathione in defense and signaling: lessons from a small thiol. *Ann. N. Y. Acad. Sci.* **973**, 488-504

Dorr, R. (1988). New fndings in the pharmacokinetic, metabolic, and drug-resistance aspects of mitomycin C. *Semin. Oncol.* **4**, 32- 41

Ernster, L. (1986). DT Diaphorase: a historical review. *Chemica Scripta.* **27A**, 1-13

Ernster, L., Danielson, L., and Ljunggren, M. 1(962). DT Diaphorase-1, purification from soluble fraction of rat-liver cytoplasm, and properties. *Biochim. Biophys. Acta*. **58**, 171-188

Ernster, L., and Navazio, F. (1958). Soluble diaphorase in animal tissues. *Acta. Chem. Scand.* **12**, 595-599

Gant, T.W., RamakrishnaRao, D.N., Mason, R.P., and Cohen, G.M. (1988). Redox cycling and sulfhydryl arylation - their relative importance in the mechanism of quinone cyto-toxicity to isolated hepatocytes. *Chemico-biological interactions.* **65**, 157-173.

Garewal, H.S. (1988). Mitomycin C in the chemotherapy of advanced breast cancer. *Semin. Oncol.* **15**, S74

Goodenough, DA and Paul, DL. (2003). Beyond the gap: functions of unpaired connexon channels. *Nat Rev Mol Cell Biol*. 4(4):285-94

Goswami, R., Kilkus, J., Dawson, S.A., Dawson, G. (1999). Overexpression of Akt (protein kinase B) confers protection against apoptosis and prevents formation of ceramide in response to pro-apoptotic stimuli. *J. Neurosci. Res.* **57**, 884-893

Gray, W., and Melanie, H. (2002). Cell Condition-dependent Regulation of ERK5 by cAMP**.** *J. Biol. Chem.* **277**, 48094 – 48098

Hargreaves, R.H., Hartley, J.A., and Butler, J. (2000). Mechanisms of action of quinone-containing alkylating agents: DNA alkylation by aziridinylquinones. *Front Biosci.* **5**, E172-E180

Henryk, D., Sandeep, R.D., Thomas, F., Franke, M.J., Birnbaum, R.Y., Geoffrey M. Cooper, Rosalind A. Segal, David R.K., and Michael, E.G. (1997). Regulation of Neuronal Survival by the Serine-Threonine Protein Kinase Akt. *Science.* **275**, 661-665

Herrlich, P., and Böhmer, F.D. (2000). Redox regulation of signal transduction in mammalian cells. *Biochem. Pharmacol.* **59**, 35-41

Huimin, W., Yong, M., Nai. Z., Tao, H., and Leroy, F.L. (2001). ATP-bound topoisomerase II as a target for antitumor drugs. *J. Biol. Chem.* **276**,15990-15995

Kato, Y.T., Huang, S., Watson, M.H., Ulevitch, R.J., Lee, J.D. (1998). Bmk1/Erk5 is required for cell proliferation induced by epidermal growth factor. *Nature.* **395**, 713-716

Kim, D.Y., Kam, Y., Koo, S.K., and Joe, C.O. (1999). Gating Connexin 43 Channels Reconstituted in Lipid Vesicles by Mitogen-activated Protein Kinase Phosphorylation *J. Biol. Chem.* **274**, 5581-5587

Willecke, K., Eiberger, J., Degen, J., Eckardt, D., Romualdi, A., Güldenagel, M., Deutsch, U., and Söhl, G. (2002). Structural and functional diversity of connexin genes in the mouse and human genome. *Biol. Chem.* **383**, 725-737

Klotz, L.O. (2002a). Oxidant-induced signaling: effects of peroxynitrite and singlet oxygen. *Biol. Chem.* **383**, 443-456

Klotz, L.O., Patak, P., Ale-Agha, N., Buchczyk, D.P., Abdelmohsen, K., Gerber, P.A., von Montfort, C., and Sies, H. (2002b). 2-Methyl-1,4-naphthoquinone, vitamin K(3), decreases

gap-junctional intercellular communication via activation of the epidermal growth factor receptor/extracellular signal-regulated kinase cascade. *Cancer Res.* **62**, 4922-4928

Klotz, L.O., Schieke, S.M., Sies, H., and Holbrook, N.J. (2000). Peroxynitrite activates the phosphoinositide 3-kinase/Akt pathway in human skin primary fibroblasts. *Biochem.J.* **352**, 219-225

Kulik, G., Klippel, A., and Weber, M.J. (1997). Antiapoptotic signalling by the insulin-like growth factor I receptor, phosphatidylinositol 3-kinase, and Akt. *Mol. Cell Biol.* **17**, 1595-1606

Lame, M.W., Jones, A.D., Wilson, D.W., Segall, H.J. (2003). Protein targets of 1,4-benzoquinone and 1,4 naphthoquinone in human bronchial epithelial cells. *Proteomics.* **3**, 479-495

Lampe, P.D., and Lau, A.F. (2000). Regulation of gap junctions by phosphorylation of connexins. *Arch. Biochem. Biophys.* **384**, 205–215

Lee, J. W., and Juliano, R. L. 2000, $_{\alpha}5^{\beta}1$ Integrin protects intestinal epithelial cells from apoptosis through a phosphatidylinositol 3-kinase and Protein kinase B-dependent pathway. *Mol. Biol. Cell.* **11**, 1973-1987

Leykauf, K., Durst, M., Alonso, A. (2003). Phosphorylation and subcellular distribution of connexin43 in normal and stressed cells. *Cell and tissue research.* **311**, 23-30

Li, X.A., Bianchi, C., and Sellke, F.W. (2001). Rat aortic smooth muscle cell density affects activation of MAP kinase and Akt by menadione and PDGF homodimer BB. *J. Surg. Res.* **100**, 197-204

Loewenstein, W.R. (1987). The cell-to-cell channel of gap-junctions. *Cell.* **48**, 725-726

Malisza, K.L., and Hasinoff, B.B. (1996). Inhibition of anthracycline semiquinone formation by ICRF-187 (dexrazoxane) in cells. *Free Radicals in Biology and Medicine.* **20**, 905-914

Marais, R., Light, Y., Paterson, H.F., and Marshall, C.J. (1995). Ras recruits Raf-1 to the plasma membrane for activation by tyrosine phosphorylation. *EMBO J.* **14**, 3136-3145.

Mayer, H., and Isler, O. (1971). Synthesis of vitamins K. *Methods in Enzymology.* Vol. **18C**, 491-547

Meister, A.A. (1983). Glutathione. *annual review of biochemistry*. **52**, 711-760

Mendelsohn, J. (2002). Targeting the epidermal growth factor receptor for cancer therapy. *Journal of Clinical Oncology.* **20** (18): 1S-13S Suppl. S

Mody, N., Leitch J., Armstrong, C., Dixon J., and Cohen P. (2001). Effects of MAP kinase cascade inhibitors on the MKK5/ERK5 pathway. *FEBS Lett.* **502**, 21-24

Mosmann, T. (1983). Rapid colorimetric assay for cellular growth and survival: Application to proliferation and cytotoxicity assays. *J. Immunol. Methods.* **95**, 55-63

Nutter, L.M., Cheng, A.L., Hung, H.L., Hsieh, R.K., Ngo, E.O., Liu, T.W. (1991). Menadione: spectrum of anticancer activity and effects on nucleotide metabolism in human neoplastic cell lines. *Biochem. Pharmacol.* **41**, 1283

Oh, S.Y., Grupen, C.G., and Murray, A.W. (1991). Phorbol ester induces phosphorylation and down-regulation of connexin 43 in WB cells. *Biochim. Biophys. Acta.* **1094**, 243–245

Olayioye, M.A., Neve, R.M., Lane, H.A., Hynes, N.E. (2000). The ErbB signaling network: receptor heterodimerization in development and cancer. *EMBO J.* **19**, 3159-3167.

Pasterz, R.B., Buzdar, A.U., Hortobagyi, G.N., and Blumenschein, G.R. (1985). Mitomycin in metastatic breast cancer refractory to hormonal and combination chemotherapy. *Cancer.* **56**, 2381

Petrich, B.G., Gong, X., Lerner, D.L., Wang, X., Brown, J.H., Saffitz, J.E., and Wang, Y. (2002) *Circ. Res.* **91**, 640–647

Polontchouk, L., Ebelt, B., Jackels, M., and Dhein, S. (2002). Chronic effects of endothelin-1 and angiotensin-II on gap junctions and intercellular communication in cardiac cells. *FASEB J.* **16**,87–89

Prenzel, N., Fischer, O.M., Streit, S., Hart, S., Ullrich, A. (2001). The epidermal growth factor receptor family as a central element for cellular signal transduction and diversification. *Endocrine-Related Cancer.* **8**, 11-31

Sako, Y., Minoghchi, S., Yanagida, T. (2000). Single-molecule imaging of EGFR signalling on the surface of living cells *Nature cell biology.* **2**, 168-172

Scott, J.C., Sundeep, M., Masashi, A., Nicole, M., Chen, Y., Jiing-Dwan, L., Jun-ichi, A., and Jay, Y. (2003). Regulation of Epidermal Growth Factor-induced Connexin 43 Gap Junction Communication by Big Mitogen-activated Protein Kinase 1/ERK5 but Not ERK1/2 Kinase Activation. *J. Biol. Chem.* **278**, 18682 - 18688.

Sharov, V. S. Briviba, K., and Sies, H. 1999, Peroxynitrite diminishes gap junctional communication: protection by selenite supplementation. *IUBMB Life.* **48**, 379-384

Reiter, R. (1997). Antioxidant action of Melatonin. *Antioxidants in disease mechnism and therapy*. Academic Press, pages 103-117

Sies, H. (1999). Gluatathione and its role in cellular functions. *Free Radicals in Biology and Medicine.* **27**, 916-921

Suttie, J.W. (1985). Vitamin-K-dependent carboxylase. *Annual review of biochemistry*, **54**, 459-477

Taggart, W.V. and Matschiner J.T. (1969). Metabolism of menadione-6,7-3h in rat. *Biochemistry.* **8**, 1141

Temme, A., Buchmann, A., Gabriel, H.D., Nelles, E., Schwarz, M., Willecke, K. (1997). High incidence of spontaneous and chemically induced liver tumors in mice deficient for connexin32. *Curr. Biol.* **9**, 713-6.

Tero, A.H., Tanner, M., Rantanen, V., Bärlund, M., Borg, Ä., Grénman, S., and Isola, J. (2000). Amplification and deletion of topoisomerase II associate with ErbB-2 amplification and affect sensitivity to topoisomerase II inhibitor doxorubicin in breast cancer. *Am. J. Pathol.* **156**: 839-847

Tetef, M., Margolin, K., et al. (1995). Mitomycin C and menadione for the treatment of advanced gastrointestinal cancers - a phase-II trial. *J. Cancer Res. Clin. Oncol.* **121**, 103

Tomasz, M., Chawala, A., and Lipman, R. (1988). Mechanism of monofunctional and bifunctional alkylation of DNA by Mitomycin C. *Biochemistry.* **27**, 3182-3187

Toon, A.B., Harold, V.M., and Opthof, T. (2001). Cardiac gap junction channels: modulation of expression and channel properties. *Cardiovascular Research*. **51**, 217– 229

Trosko, J.E., and Ruch, R.J. (1998). Cell-cell communication in carcinogenesis. *Front Biosci.* **3**, D208–D236

Unger, V.M., Kumar, N.M., Gilula, N.B., and Yeager, M. (1999). Three-dimensional structure of a recombinant gap junction membrane channel. *Science.* **283**, 1176–1180

Waidyanatha, S., Troester, M.A., Lindstrom, A.B., Rappaport, S.M. (2002). Measurement of hemoglobin and albumin adducts of naphthalene-1,2-oxide, 1,2-naphthoquinone and 1,4-naphthoquinone after administration of naphthalene to F344 rats *Chemico-biological interactions.* **141**, 189-210

Wang, X., McCullough, K.D., Franke, T.F., and Holbrook, N.J. (2000). Epidermal Growth Factor Receptor-dependent Akt Activation by Oxidative Stress Enhances Cell Survival. *J. Biol. Chem.* **275**, 14624-14631

Warn-Cramer, B.J., Paul D.L., Wendy, E.K., Martha, Y., Kanemitsu, Lenora, W.M. L., Walter E., and Alan F.L. (1996). Characterization of the Mitogen-activated Protein Kinase Phosphorylation Sites on the Connexin-43 Gap Junction Protein. *J. Biol. Chem.* **271**, 3779 – 3786

Whitmarsh, A.J. and Davis, R J. (2000). A central control for cell growth. *Nature.* **403**, 255-256

Wu, R.C., Hohenstein, A., Park, J.M., Qiu, X., Mueller, S., Cadenas, E., and Schönthal, A.H. (1998). Role of p53 in aziridinylbenzoquinone-induced p21waf1 expression. *Oncogene.* **17**, 357-365

Wu, W., Graves, L.M., Jaspers, I., Devlin, R.B., Reed, W., and Samet, J.M. (1999). Activation of the EGF receptor signaling pathway in human airway epithelial cells exposed to metals. *Am. J. Physiol.* **277**, L924-L931

Erklärung

Hiermit erkläre ich, daß ich die vorliegende Dissertation eigenständig und ohne unerlaubte Hilfe angefertigt und diese in der vorliegenden oder in ähnlicher Form noch bei keiner anderen Institution eingereicht habe.

(Kotb Abdelmohsen)

……..

Düsseldorf, 20. Oktober 2003